CIGS The Canon Institute for Global Studies

CIGS Working Paper Series No. 26-007E

State Dependence of Monetary Policy During Global Supply Chain Disruptions

Xiwen Bai (Tsinghua University)
Jes´us Fern´andez-Villaverde (University of Pennsylvania,)
Yiliang Li (University of International Business and Economics)
Francesco Zanetti (University of Oxford)

May, 2026

General Incorporated Foundation
The Canon Institute for Global Studies
一般財団法人 キヤノングローバル戦略研究所
Phone: +81-3-6213-0550 https://cigs.canon/

State Dependence of Monetary Policy During Global Supply Chain Disruptions*

Xiwen Bai† Jesús Fernández-Villaverde‡ Yiliang Li§

Francesco Zanetti¶

May 2026

Abstract

We study how global supply chain disruptions affect monetary policy transmission. Post-pandemic evidence indicates surging transportation costs, goods-market imbalances, and rising prices. We develop a model in which logistical bottlenecks (upstream slack coexisting with downstream shortages) steepen the aggregate supply curve. This convexity amplifies price responses to monetary policy while dampening output effects. Threshold VAR and Local Projection estimates are consistent with this mechanism: during disruptions, contractionary policy reduces prices more at smaller output cost, easing the stabilization trade-off.

JEL Classification: C32, E31, E32, E52.
Keywords: Monetary Policy, Supply Chain Disruption, State Dependence, Convex Supply Curve, Inflation.

*We thank Anil Kashyap, Veronica Guerrieri, Sarah Zubairy and participants at numerous conferences and seminars for extremely helpful comments and suggestions. Francesco Zanetti gratefully acknowledges the hospitality of the Hong Kong Monetary Authority.
† Bai: Tsinghua University, China. xiwenbai@mail.tsinghua.edu.cn. ‡ Fernández-Villaverde: University of Pennsylvania, U.S. jesusfv@econ.upenn.edu. § Li: University of International Business and Economics, China. yiliang_li@uibe.edu.cn. ¶ Zanetti: University of Oxford, U.K. francesco.zanetti@economics.ox.ac.uk.

1. Introduction

Global supply chains are central to modern production, and any major disruption, such as the halt to international trade at the onset of the COVID-19 pandemic in 2020, can generate sharp adjustments in domestic prices, even when local economic conditions remain benign. Indeed, such disruptions played a prominent role in driving U.S. inflation to unprecedented levels, peaking near 9% in 2022, following over two decades of low and stable inflation of around 2.5%. Given central banks' mandate for price stability, should monetary policy adjust its stance forcefully to address the sudden and sharp price increases amid supply chain disruptions? In other words, do global supply chain disturbances alter the trade-offs policymakers face, and should monetary policy adopt a different response?

In this paper, we highlight important interrelated facts connecting global supply chain disruptions to domestic conditions in the U.S. between 2017 and 2023, showing that such disruptions were associated with elevated transportation costs, severe imbalances in the supply and demand for goods, and a surge in goods prices. We develop a simple model that incorporates these empirical regularities by accounting for upstream production slack and downstream supply shortages simultaneously. The model demonstrates analytically that supply chain disruptions, which curtail the availability of goods in retail markets, increase the convexity of the aggregate supply curve. As a result, adjustments in demand driven by monetary policy during disruptions lead to significant price changes with limited effects on real output. Estimates from both structural Threshold Vector Autoregression (TVAR) and Local Projection (LP) models are consistent with this mechanism, revealing significant state-dependent effects of monetary policy during periods of global supply chain disruptions.

We begin by documenting three stylized facts concerning the post-pandemic economic recovery that motivate our subsequent theoretical framework. Fact I demonstrates that global supply chain disruptions, identified using the Average Congestion Rate (ACR) of container ships at major ports worldwide, result in a significant increase in transportation costs.[1] Fact II shows that such disruptions coincide with substantial imbalances between U.S. demand and the spare productive capacity of major U.S. trading partners. Fact III documents that the resulting tightening of product markets coincided with rapid goods-price inflation.

[1]The ACR index in Bai et al. (2024) is constructed using satellite-based Automatic Identification System (AIS) data of container ships and a specialized density-based spatial clustering algorithm (Bai et al., 2023).

Next, we develop a parsimonious model —building on Michaillat and Saez (2015), Ghassibe and Zanetti (2022), and Bai et al. (2024)— that incorporates the empirical regularities documented in Facts I-III while maintaining tractability to analytically study the state-dependent effects of monetary policy. The model features search frictions between producers and retailers, as well as transportation costs. Search frictions disrupt the allocative role of prices, as the costs of searching influence the balance between demand and supply, generating spare productive capacity for producers alongside supply shortages for retailers. Transportation costs further constrain the delivery of goods, amplifying upstream production slack while exacerbating downstream supply shortages and driving sharp price increases in the retail market.

Crucially, we demonstrate analytically that supply chain disruptions, modeled as an unexpected surge in transportation costs, do not merely curtail the level of supply; they fundamentally alter the slope of the aggregate supply curve. This steepening arises from the changing nature of the "margin" —specifically, the density of producer-retailer matches that are just barely profitable at the reservation transportation cost. In normal times, a small increase in the acceptable price covers the transportation costs for a large volume of potential matches, keeping the supply curve relatively flat. However, during a global supply chain disruption, transportation costs increase substantially, and the formation of profitable producer–retailer matches diminishes significantly at the margin. Consequently, a large price premium is required to cover transportation costs, and the number of matches declines, thereby curbing the volume of aggregate supply. In other words, global supply chain disruptions make the aggregate supply curve locally convex: during disruptions, prices become highly sensitive to changes in demand, whereas output becomes relatively inelastic.

This result addresses a critical distinction in the literature regarding the source of supply convexity. While Boehm and Pandalai-Nayar (2022) identify convexity arising from physical capacity constraints (where plants approach maximum utilization), and Benigno and Eggertsson (2023) attribute it to labor market tightness, our model isolates the role of *logistical* frictions. Importantly, we show that transportation bottlenecks can steepen the aggregate supply curve and inhibit quantity adjustments even when producers possess spare productive capacity (Fact II). This implies that producer–retailer search frictions generate convexity in the supply of goods, which is important for identifying the underlying state of the economy and the appropriate policy response.

Subsequently, we complement our theoretical analysis with empirical evidence from the U.S. economy during 2017-2023. Using a structural TVAR and LPs conditioned on the ACR index, we examine the co-movement of prices and output following monetary policy shocks. We interpret these empirical results with caution given the short sample size and the presence of concurrent shocks during the post-pandemic recovery. Rather than a definitive test, we view the analysis as providing suggestive evidence consistent with our theoretical mechanism.

The estimates indicate that during periods of supply chain disruption, contractionary monetary policy is associated with a significantly stronger and more persistent decline in goods prices than in output.[2] Specifically, in the TVAR model, the impact decline in U.S. goods prices nearly doubles, from approximately -0.1% to -0.2%, with the shock's persistence extending from around 6 months to over 12 months. The results from the LP model are fully consistent with the TVAR findings. An extensive sensitivity analysis confirms the robustness of these results across several dimensions, including the use of congestion times to gauge the state of the global supply chain and variations in identification restrictions and model specifications.

The policy implications of our analysis extend beyond the COVID-19 recession and resonate with a long tradition in economics, dating back to John Maynard Keynes. Keynes (1940) argued that when output is constrained —at the time due to resources diverted to support wartime activities during World War II— policymakers should not hesitate to forcefully restrain aggregate demand in order to prevent price escalation without significantly harming production. Our theoretical and empirical results underpin Keynes's original argument.

Related literature. Our study is linked to three strands of literature. First, our theoretical framework builds on studies that develop tractable models with convex supply curves, illustrating their relevance for prices and fiscal policy (Michaillat and Saez, 2015, 2022; Boehm and Pandalai-Nayar, 2022; Ghassibe and Zanetti, 2022, respectively).

Second, our analysis builds on studies that examine the state-dependent effects of monetary policy across dimensions other than supply chain disruptions. Important factors include the distribution of savings from mortgage refinancing (Berger et al., 2021; Eichenbaum et al., 2022);

[2]The identification restrictions in the TVAR model, guided by our theoretical predictions, specify that a contractionary monetary policy shock generates negative impact responses in real GDP, the PCE goods price, product market tightness, and import prices; positive impact responses in the spare capacity rate and the federal funds rate; and a zero impact response in the ACR index. The LP model adopts a similar set of sign restrictions extended to longer horizons, but excludes the restriction on the ACR index and imposes an additional elasticity bound on the impact response of real GDP.

financial frictions (Bernstein, 2021); downward nominal wage rigidities (Benigno and Ricci, 2011); the attentiveness of depositors to interest rates (Eichenbaum et al., 2025); recessionary and non-recessionary states of the business cycle (Tenreyro and Thwaites, 2016; Angrist et al., 2018); household heterogeneity (Lippi et al., 2015; Bilbiie et al., 2023); the effective lower bound on short-term nominal interest rates (Liu et al., 2019; Ikeda et al., 2024); household net worth levels (Harding and Klein, 2022); credit and interest rate cycles (Alpanda et al., 2021); and interactions with oil supply news shocks (Miyamoto et al., 2024; Verduzco-Bustos and Zanetti, 2026).

Third, our work relates to studies examining the aggregate implications of supply chain disturbances during the COVID-19 pandemic, focusing on the role of spare labor and productive capacity (Benigno and Eggertsson, 2023; Bai et al., 2024, respectively), labor and goods shortages (di Giovanni et al., 2022, 2023; Bernanke and Blanchard, 2025), quasi-kinked demand curves for produced goods (Harding et al., 2023), and productive capacity constraints (Balleer and Noeller, 2023; Comín et al., 2023).

The remainder of the paper is organized as follows. Section 2 documents three stylized facts linking global supply chain disruptions to transportation costs, imbalances in the supply and demand for goods, and changes in U.S. goods prices. Section 3 outlines the theoretical model and derives analytical predictions regarding the state-dependent effects of monetary policy. Section 4 examines the consistency of these predictions with the data using both a structural TVAR model and an LP model with interaction terms. Section 5 concludes. The appendix provides additional details, including proofs, estimation specifications, and robustness checks.

2. Motivating Facts

This section presents descriptive evidence characterizing the economic environment of the post-pandemic recovery. We document three stylized facts linking global supply chain disruptions to transportation costs, imbalances between goods supply and demand, and goods price inflation in the U.S. during the sample period from January 2017 to September 2023.

While we interpret these patterns as strongly suggestive of supply chain constraints interacting with robust demand, we acknowledge that this period was characterized by multiple concurrent shocks, including fiscal stimulus, sectoral reallocation of consumption, and labor supply shifts (Ferrante et al., 2023; Stock and Watson, 2025). Nevertheless, these facts motivate the core

mechanism of our theory in Section 3, which shows that supply chain disruptions create state-dependent trade-offs for monetary policy. They also guide the construction of new time series on global spare capacity and product market tightness, which are essential for the empirical analysis in Section 4.

Fact I: Supply Chain Disruptions and Rise in Transportation Costs

The first key feature of the post-pandemic period was the coincidence of severe logistical bottlenecks with soaring transportation costs. Bai et al. (2024) construct the ACR index of container ship congestion at major ports worldwide, which serves as a high-frequency proxy for the operational state of the global supply chain.[3]

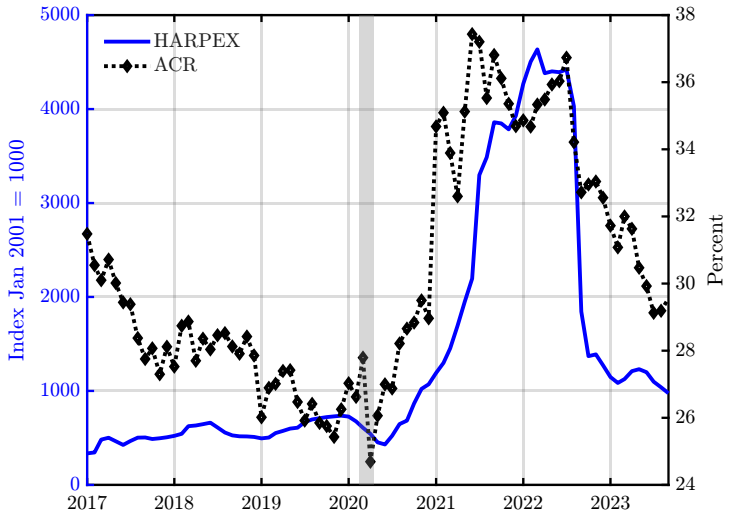

Figure 1: Port Congestion and Transportation Costs

Notes. The figure compares the ACR index, derived from AIS data using the IMA-DBSCAN algorithm (Bai et al., 2023), with the HARPEX index. The ACR index is expressed as a percentage; HARPEX is in the original units. Both series are seasonally adjusted. Gray-shaded areas represent NBER recessions.

Figure 1 plots the ACR index alongside the Harper Peterson Time Charter Rates Index (HARPEX), a benchmark for global shipping costs. The correlation illustrates a tight link between physical congestion and the price of shipping services. As port congestion escalated, the effective supply of shipping capacity contracted, triggering a sharp rise in seaborne transportation costs (see also Bai et al., 2025). This relationship underscores that the "supply chain shock" was

[3]Estimates show that COVID-19-related port congestion surged in late 2020 and persisted through mid-2022, with the share of delayed ships rising from 28% to 37% and average delays more than doubling. Given the indirect nature of global shipping networks (Ganapati et al., 2024), these delays cascaded through the supply chain.

not merely a quantity constraint but a cost shock, compounded by the highly concentrated nature of the container shipping industry (UNCTAD, 2022).

Fact II: Significant Imbalances in Supply and Demand for Goods

The second fact highlights the macroeconomic mismatch that defined the recovery: a strong recovery in domestic goods demand colliding with limited global spare capacity. To capture this imbalance, we compare U.S. manufacturers' new orders (a proxy for goods demand) with a novel measure of the import-weighted average spare capacity of major U.S. trading partners (a proxy for global production slack).[4] We construct the spare capacity as:

$$\text{SpareCapacityDollar}_t = \sum_{i \in \mathscr{C}} \left[\frac{\text{Import}_{i,t}}{\sum_{j \in \mathscr{C}} \text{Import}_{j,t}} \cdot \left(\frac{\text{IP}_{i,t}}{\text{CapacityUtilization}_{i,t}} - \text{IP}_{i,t} \right) \right], \tag{1}$$

where $\mathscr{C}$ denotes the set of trading partners, $\text{Import}_{i,t}$ represents U.S. goods imports by customs basis from country i, $\text{CapacityUtilization}_{i,t}$ is the country's capacity utilization rate, and $\text{IP}_{i,t}$ is industrial production in U.S. dollars.[5] This measure captures the physical slack available in the global production network to meet U.S. demand for goods.

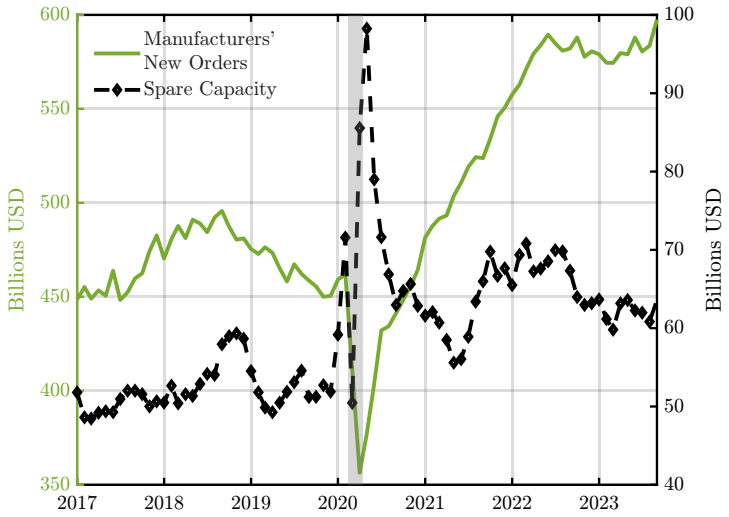

Figure 2: Imbalances in the Supply and Demand for Goods

Notes. The figure compares U.S. manufacturers' new orders with the import-weighted average spare capacity of major U.S. trading partners calculated via Equation (1). Both series are in billions of U.S. dollars and seasonally adjusted.

Figure 2 illustrates the divergence. Following the pandemic onset, U.S. new orders (solid green

[4] We focus on Mexico, Canada, China, Germany, and Japan, which account for over half of U.S. goods imports.
[5] Appendix C provides detailed definitions and descriptions of the data sources for all series used in our analysis.

line) surged, driven by a reallocation of consumption from services to goods and significant fiscal support (Guerrieri et al., 2022; Stock and Watson, 2025). Simultaneously, global spare capacity (dashed line) contracted sharply before rebounding, yet remained insufficient to close the gap with soaring demand. This persistent wedge between orders and capacity indicates that the U.S. economy was operating in a regime of acute product-market tightness.[6]

Fact III: Tightening of Product Market and Surge in Goods Prices

The final fact connects these real imbalances to nominal outcomes. We summarize the supply-demand mismatch in a single metric of product market tightness, defined as the ratio of new orders to spare capacity:

$$\text{Tightness}_t = \frac{\text{ManufactureNewOrder}_t}{\text{SpareCapacityDollar}_t}. \tag{2}$$

Figure 3 plots this tightness measure alongside the U.S. PCE goods price index. The correlation is striking. As product market tightness spiked in early 2020 and remained elevated through 2022, goods prices surged, rising approximately 15% above pre-pandemic levels.

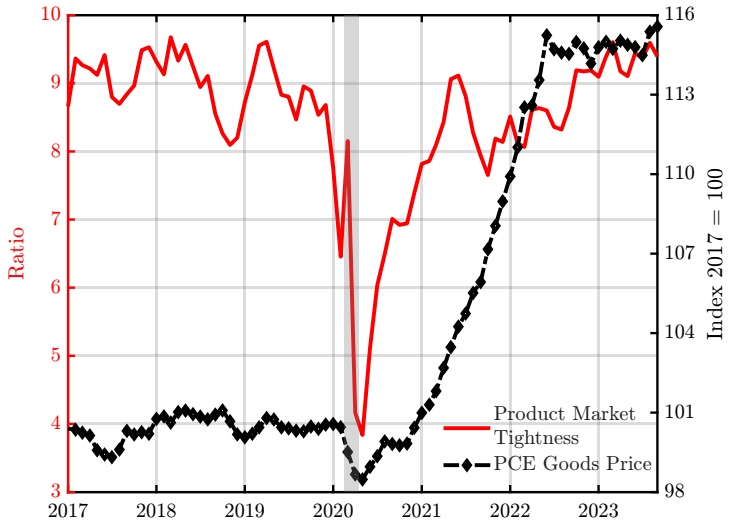

Figure 3: Co-Movements Between Goods Prices and Product Market Tightness

Notes. The figure compares the U.S. PCE goods price with the product market tightness measure from Equation (2). Both series are seasonally adjusted.

This strong positive co-movement marks a departure from the pre-pandemic business cycle. Before the pandemic, demand expansions were typically accommodated by increasing production

[6]In Appendix D, we show that these results are robust to using U.S. retailers' new orders as an alternative proxy for goods demand. Furthermore, constructing our product market tightness measure (Fact III) using this alternative series yields dynamics consistent with those reported in Figure 3.

using available spare capacity, resulting in muted price responses (Comín et al., 2023). In contrast, the post-pandemic synchronization of rising tightness and prices indicates that supply chain disruptions forced the market to clear primarily through prices rather than quantities —a feature central to the convex supply curve we model in Section 3.

Taking Stock

In summary, the descriptive evidence points to a post-pandemic economy defined by: (i) logistic constraints raising transportation costs; (ii) a persistent mismatch between global spare capacity and domestic goods demand; and (iii) resulting inflationary pressures in the goods sector. While other factors, such as labor supply shocks and fiscal policy, undoubtedly played a role, these specific supply chain dynamics form the empirical basis for the theoretical framework we develop next.

3. Theoretical Prediction

Our theory builds on the disequilibrium framework of Michaillat and Saez (2015), Ghassibe and Zanetti (2022), and Bai et al. (2024), adapting the analysis to study the impact of monetary policy on prices and output under varying severities of supply chain disruptions.

The model economy consists of producers, retailers, households, and a monetary authority that influences aggregate demand by controlling the nominal quantity of money.[7] Producers are geographically separated from retailers and households; they manufacture goods using a fixed endowment and incur transportation costs to deliver these goods to retailers (Fact I). Retailers purchase goods subject to search frictions, which prevent perfect matching with producers and lead to the occurrence of both upstream slack and downstream shortages (Fact II). These frictions give rise to product market tightness —a measure of the imbalance between supply and demand that accounts for the price surges (Fact III). Finally, retailers sell goods to households, who own

[7]We treat monetary policy as exogenous to maintain analytical tractability and to isolate the mechanism through which supply chain disruptions alter the transmission of nominal demand shocks. We acknowledge that systematic monetary policy rules can influence the slope of the aggregate demand curve and the propagation of shocks (Gagliardone and Gertler, 2023; Giannone and Primiceri, 2024). However, our analysis focuses on the convexity of the aggregate supply curve —driven by search frictions and transportation costs— which determines the split of nominal spending between prices and output, regardless of the specific reaction function generating that spending.

the producers and retailers and accrue all profits from trade.[8]

This tractable framework allows us to derive analytical solutions in the form of comparative statics to investigate whether supply chain disruptions alter the stabilization trade-off of monetary policy between controlling price increases and minimizing output losses, thereby making its efficacy dependent on the state of the global supply chain.

3.1. Producers and Retailers

The economy comprises an exogenous unit mass of producers and an endogenous measure of retailers. When matched, a producer employs its fixed-factor endowment to produce $y = l$ units of the final good. Transactions occur in a frictional market, which constrains producers from selling their full productive capacity. In each period, every unmatched retailer (denoted by subscript U) visits one unmatched producer, incurring a fixed search cost $\rho > 0$ per unit of the final good for each visit. If a match is formed, the retailer purchases the goods and resells them to households at price p.

Matching function. The matching function determines the number of successful trades. In each period, the number of meetings ($\mathscr{M}$) between unmatched producers, x_U, and unmatched retailers, i_U, is determined by a constant-returns-to-scale matching function:

$$\mathscr{M} = (x_U^{-\xi} + i_U^{-\xi})^{-\frac{1}{\xi}}, \tag{3}$$

where ξ is the elasticity of substitution between x_U and i_U. We assume $\xi > 0$ such that $\mathscr{M} \leq \min\{x_U, i_U\}$, which is a necessary property of a matching function.

We define product market tightness faced by individual firms as the ratio of the number of visits by unmatched retailers to the number of unmatched producers, i.e.,

$$\theta \equiv \frac{i_U}{x_U}.$$

The probability for a producer to meet a retailer is:

$$f(\theta) = \frac{\mathscr{M}}{x_U} = (1 + \theta^{-\xi})^{-\frac{1}{\xi}}, \tag{4}$$

[8] As highlighted in Bai et al. (2024), the spatial separation of producers and retailers captures the complexities of global supply chains, where search frictions complicate trade. Transportation costs and search frictions also impede the efficient allocation of goods between producers and retailers through pricing mechanisms.

and the probability for a retailer to meet a producer is:

$$q(\theta) = \frac{\mathscr{M}}{i_U} = (1 + \theta^{\xi})^{-\frac{1}{\xi}}. \tag{5}$$

Equations (4) and (5) imply that $f'(\theta) > 0$ and $q'(\theta) < 0$. Therefore, product market tightness increases (decreases) the probability of a producer (retailer) meeting a retailer (producer).

Transportation cost. Consistent with Fact I in Section 2, producers incur transportation costs when shipping goods to retailers.[9] Each period, producers draw a per-unit transportation cost z from a log-normal distribution $G(z)$, characterized by the scale parameter γ and shape parameter σ. Specifically, $G(z) \equiv \Phi\left[(\ln z - \gamma)/\sigma\right]$, where $\Phi(\cdot)$ represents the standard normal c.d.f.[10] As discussed later, there exists a cut-off transportation cost $\bar{z}$, beyond which matches become unprofitable and are terminated ($z > \bar{z}$), while matches remain viable when $z \leq \bar{z}$.

Value functions. At the start of each period, matched producers sell their goods to retailers at the wholesale price and incur transportation costs. Matched retailers then resell these goods to households at the retail price. Simultaneously, unmatched producers and retailers search for trading partners in the product market. Upon entering the subsequent period, each producer draws a new transportation cost; matches are sustained only if this cost is sufficiently low to generate a positive trade surplus.

Four value functions describe the returns for the various statuses of producers and retailers. The value function for a matched producer (denoted by the subscript M), $X_M(z)$, is given by:

$$X_M(z) = (r(z) - z)\, l + \beta \int_0^{+\infty} \max\left(X_M(z'), X_U\right) dG(z'), \tag{6}$$

where $r(z)$ represents the (endogenous) wholesale price per unit of the final good, β is the discount factor, and z' is the transportation cost drawn at the start of the next period. Equation (6) establishes that the value for a matched producer comprises the current profit, $(r(z) - z)\, l$, and the expected continuation value. The latter depends on the persistence of the match, which is contingent on the transportation cost z' drawn in the subsequent period. The max operator captures the optimal decision to either sustain the match or separate.

[9] For simplicity, we assume that the households receive such costs as payment for moving the goods.
[10] Refer to Bai et al. (2024) for a detailed explanation of the transportation cost modeling choice.

The value for an unmatched producer, X_U, is:

$$X_U = \beta f(\theta) \int_0^{+\infty} \max\left(X_M(z'), X_U\right) dG(z') + \beta\left(1 - f(\theta)\right) X_U. \tag{7}$$

With probability $f(\theta)$, an unmatched producer encounters a retailer but may forego the match if the newly drawn transportation cost renders trade unprofitable. Conversely, with probability $1 - f(\theta)$, the producer fails to secure a partner and remains unmatched into the next period.

The value for a matched retailer, $I_M(z)$, is:

$$I_M(z) = \left(p - r(z)\right) l + \beta \int_0^{+\infty} \max\left(I_M(z'), I_U\right) dG(z'). \tag{8}$$

A matched retailer resells each unit of the good to households at price p while paying the wholesale price $r(z)$ to the producer. Analogous to the producer's problem, the max operator captures the optimal decision to either sustain the match or separate, contingent on the transportation cost z' realized in the subsequent period.

If the drawn transportation cost makes the match unprofitable, the retailer separates from the match and starts the next period with a return:

$$I_U = -\rho l + \beta q(\theta) \int_0^{+\infty} \max\left(I_M(z'), I_U\right) dG(z') + \beta\left(1 - q(\theta)\right) I_U, \tag{9}$$

where ρ is a fixed cost per unit of the final good that the retailer pays to the producer during the visit. Free entry into the product market drives the value for an unmatched retailer to zero in equilibrium, i.e., $I_U = 0$.

Surplus sharing. The total surplus generated by the match between the producer and the retailer is split according to the Nash bargaining solution. The total surplus is defined as:

$$S(z) = X_M(z) - X_U + I_M(z) - I_U. \tag{10}$$

The producer is allocated a fraction η of this surplus, while the retailer receives the remainder $1 - \eta$, yielding the following equilibrium condition:

$$\eta\left(I_M(z) - I_U\right) = (1 - \eta)\left(X_M(z) - X_U\right). \tag{11}$$

By substituting the value functions (6), (7), and (8), alongside the free-entry condition $I_U = 0$, into the Nash bargaining rule (11), the wholesale price that splits the total surplus is:

$$r(z) = \eta(p + \rho\theta) + (1 - \eta)z.$$

This expression demonstrates that the wholesale price converges to the transportation cost z as the producer's bargaining power vanishes ($\eta \to 0$). The trading externality, captured by product market tightness θ, weakens the retailers' bargaining position by reducing their matching probability. Consequently, the wholesale price is an increasing function of market tightness.

Match separation and creation. The transportation cost z reduces the joint value of a matched pair, $X_M(z) + I_M(z)$, leading to the existence of a reservation transportation cost $\bar{z}$. When transportation costs exceed this threshold, the resulting negative surplus triggers the severance of the match. This threshold is defined where the total surplus in Equation (10) vanishes:

$$S(\bar{z}) = 0. \tag{12}$$

By substituting the value functions (6), (7), and (8), along with the free-entry condition $I_U = 0$, into Equation (12), we obtain the match separation condition:

$$\mathbb{F}(p, \bar{z}, \theta) = (p - \bar{z})\, l + (1 - \eta f(\theta))\, \beta \int_0^{\bar{z}} S(z')dG(z') = 0. \tag{13}$$

Furthermore, using the value function for an unmatched retailer (9) and the free-entry condition $I_U = 0$, the match creation condition is defined as:

$$\mathbb{H}(\bar{z}, \theta) = \frac{\rho l}{q(\theta)} - (1 - \eta)\beta \int_0^{\bar{z}} S(z')dG(z') = 0, \tag{14}$$

which equates the retailer's current search cost to the expected discounted surplus from a successful match.

Aggregate supply. Aggregate supply in the economy represents the volume of goods traded by producer-retailer pairs that remain matched, given a productive capacity equal to the factor endowment l. To characterize the supply side, we consider the law of motion for the number of matched producers at the beginning of the next period, x'_M:

$$x'_M = G(\bar{z})x_M + f(\theta)G(\bar{z})x_U,$$

and for the number of unmatched producers:

$$x'_U = [1 - f(\theta) + f(\theta)\,(1 - G(\bar{z}))]\,x_U + (1 - G(\bar{z}))\,x_M.$$

Applying the identity $x_M + x_U = 1$, the law of motion for matched producers simplifies to:

$$x'_M = f(\theta)G(\bar{z}) + (G(\bar{z}) - f(\theta)G(\bar{z}))\,x_M. \tag{15}$$

Aggregate supply is thus the total output produced by the number of active matches:

$$c_s(\bar{z}, \theta) = x_M(\bar{z}, \theta)l. \tag{16}$$

3.2. Representative Household and Monetary Policy

The representative household derives utility from consumption and real money balances:

$$u\left(c, \frac{m}{p}\right) = \frac{\chi}{1+\chi} c^{\frac{\varepsilon-1}{\varepsilon}} + \frac{1}{1+\chi}\left(\frac{m}{p}\right)^{\frac{\varepsilon-1}{\varepsilon}},$$

where c denotes consumption, m is the nominal money balance, and p is the retail price. The parameter $\chi > 0$ weights the preference for consumption relative to real balances, while $\varepsilon > 1$ represents the elasticity of substitution between the two. The monetary authority controls the money supply, which determines the nominal money balance and dictates aggregate demand for a given price level, as we demonstrate below.

The household owns both producers and retailers, receiving lump-sum profit rebates and the transportation costs paid by producers as compensation for delivering goods. To maximize utility at a given price level, the household chooses its consumption and nominal money balance, subject to the following budget constraint:

$$pc + m \leq \mu + pc_s(\bar{z}, \theta) - \rho l i_U,$$

where $\mu > 0$ is the household's endowment of nominal money, $c_s(\bar{z}, \theta)$ is the aggregate supply as defined in Equation (16), and $\rho l i_U$ represents the aggregate search outlay borne by unmatched retailers. Solving the household's optimization problem yields the optimality condition:

$$\frac{\chi}{1+\chi} c^{-\frac{1}{\varepsilon}} = \frac{1}{1+\chi}\left(\frac{m}{p}\right)^{-\frac{1}{\varepsilon}}. \tag{17}$$

Aggregate demand and monetary policy. Aggregate demand represents the level of consumption that maximizes utility for a given price level when the money market clears —a condition that holds both in and out of equilibrium. Substituting $m = \mu$ into the optimality condition (17) and rearranging yields:

$$c_d(p) = \chi^{\varepsilon} \frac{\mu}{p}, \tag{18}$$

which is strictly decreasing and convex in p on $(0, +\infty)$. An increase in the price level reduces the real value of money holdings; to restore the optimal marginal rate of substitution between consumption and real balances, the household must reduce its consumption. Consequently, the aggregate demand curve is downward-sloping. Furthermore, the monetary authority directly influences aggregate demand by adjusting the nominal money supply μ. For instance, a contractionary policy that reduces μ shifts the demand curve inward.

3.3. Equilibrium and Steady State

We proceed by defining the equilibrium for a single period and the corresponding steady state.[11]

Definition 1. *A period equilibrium is defined by a price p, a reservation transportation cost $\bar{z}$, and a product market tightness θ that simultaneously satisfy the match separation condition (13) and the match creation condition (14):*

$$\mathbb{F}(p, \bar{z}, \theta) = \mathbb{H}(\bar{z}, \theta) = 0,$$

along with the market clearing condition for the downstream retailer–household market:

$$c_s(\bar{z}, \theta) = c_d(p).$$

Here, aggregate supply $c_s(\bar{z}, \theta)$ is determined by the law of motion for matched producers given in Equation (15).

Our identifying restrictions are based on steady state analysis, and we study them using comparative statics (Section 3.4). Imposing $x'_M = x_M$ on Equation (15) yields the steady-state

[11] For simplicity, we characterize the equilibrium period-by-period rather than outlining the full sequential equilibrium path. This can be interpreted as the set of prices and allocations at time t, conditional on the history of shocks.

mass of matched producers:

$$x_M^{ss}(\bar{z},\theta) = \frac{f(\theta)G(\bar{z})}{1-G(\bar{z})+f(\theta)G(\bar{z})}.$$

Consequently, the steady-state aggregate supply represents the output provided by this mass of producers, given the productive capacity l:

$$c_s^{ss}(\bar{z},\theta) = x_M^{ss}(\bar{z},\theta)l = \frac{f(\theta)G(\bar{z})}{1-G(\bar{z})+f(\theta)G(\bar{z})}\, l. \tag{19}$$

Definition 2 formalizes the steady state, while Proposition 1 confirms its unique existence.

Definition 2. *The steady state corresponds to a tuple $(p^*, \bar{z}^*, \theta^*)$ that jointly satisfies the match separation condition $\mathbb{F}(p,\bar{z},\theta) = 0$, the match creation condition $\mathbb{H}(\bar{z},\theta) = 0$, and the retailer–household market clearing condition $c_s^{ss}(\bar{z},\theta) = c_d(p)$, specifically:*

$$\frac{f(\theta)G(\bar{z})}{1-G(\bar{z})+f(\theta)G(\bar{z})}\, l = \chi^{\varepsilon}\frac{\mu}{p}. \tag{20}$$

Proposition 1. *There exists a unique steady state $(p^*, \bar{z}^*, \theta^*)$ such that the conditions for match separation, match creation, and retailer–household market clearing hold simultaneously.*

Proof. See Appendix E.1 in Bai et al. (2024). ■

With the existence and uniqueness of the steady state confirmed, we proceed to characterize the steady-state aggregate supply schedule $p \mapsto c_s^{ss}(p)$. This schedule is derived from the partial equilibrium in the upstream producer–retailer market —where $\mathbb{F}(\bar{z},\theta;p) = \mathbb{H}(\bar{z},\theta) = 0$ hold for a fixed p. The following proposition details its properties.

Proposition 2. *For any $\bar{z} \geq \bar{z}_{\min}$, where the lower bound $\bar{z}_{\min}$ is defined by:*

$$\int_0^{\bar{z}_{\min}} G(z')\, dz' = \frac{\rho}{(1-\eta)\beta}, \tag{21}$$

the steady-state aggregate supply schedule $p \mapsto c_s^{ss}(p)$, arising from the partial equilibrium in the upstream market, exhibits the following properties:

1. *The mapping*

$$\bar{z} \mapsto p(\bar{z}) \equiv \bar{z} - (1-\eta f(\bar{z}))\,\beta \int_0^{\bar{z}} G(z')\, dz',$$

is continuously differentiable and strictly increasing, with:

$$f(\bar{z}) = \left(1 - q(\bar{z})^{\xi}\right)^{\frac{1}{\xi}}, \quad q(\bar{z}) = \frac{\rho}{(1-\eta)\beta \int_0^{\bar{z}} G(z')\, dz'}.$$

Accordingly, there exists a unique, continuously differentiable steady-state aggregate supply curve $p \mapsto c_s^{ss}(p)$, defined parametrically by $(p(\bar{z}), c_s^{ss}(\bar{z}))$ for $\bar{z} \in [\bar{z}_{\min}, +\infty)$;

2. *The supply bounds are $\lim_{p \to p_{\min}} c_s^{ss}(p) = 0$ and $\lim_{p \to +\infty} c_s^{ss}(p) = l$, where the minimum price $p_{\min}$ is given by:*

$$p_{\min} \equiv \bar{z}_{\min} - \beta \int_0^{\bar{z}_{\min}} G(z')\, dz' = \bar{z}_{\min} - \frac{\rho}{1-\eta}; \tag{22}$$

3. *The function $c_s^{ss}(p)$ is strictly increasing in p over the domain $[p_{\min}, +\infty)$ and converges asymptotically to a constant as $p \to +\infty$;*

4. *The curvature of $c_s^{ss}(p)$ is locally convex near $p_{\min}$ if $\xi \in (0,1)$, linear if $\xi \geq 1$, and becomes strictly concave for sufficiently high p.*

Proof. See Appendix E.2 in Bai et al. (2024). ■

Proposition 2 states that aggregate supply is an increasing function of price due to two complementary channels. First, higher prices enhance the surplus generated by producer–retailer matches; this incentivizes retailer search effort, thereby elevating product market tightness and the probability of match formation. As the number of matches grows, aggregate supply expands. Second, higher prices support a higher reservation transportation cost, sustaining matches that would otherwise be severed, which further boosts supply. Despite the capacity constraints imposed by search frictions and transportation costs —which generate spare capacity— the model maintains the conventional positive slope of the aggregate supply curve.

Panel 4a in Figure 4 shows the steady-state outcome in the downstream retailer-household market within the (c, p)-plane. The steady state is pinpointed by the intersection of the aggregate demand schedule and the steady-state aggregate supply schedule. The supply curve c_s^{ss} (shown in blue) exhibits a positive slope, consistent with standard theory. The gap between the total productive capacity and actual output, $l - c_s^{ss}$, represents spare capacity, capturing the combined inefficiencies arising from search frictions and transportation costs.

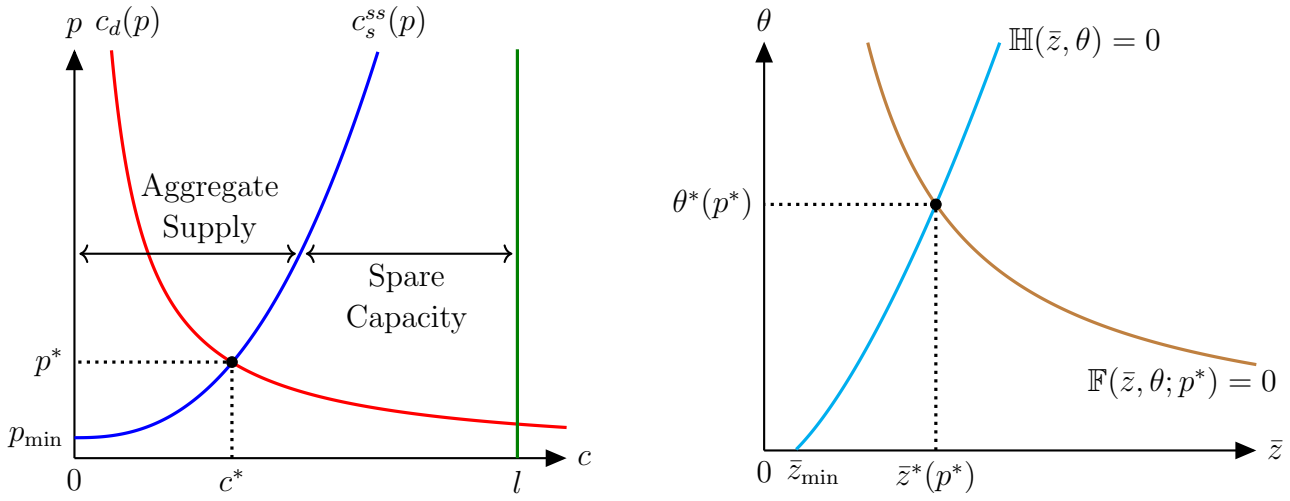

(a) Aggregate Supply and Demand

(b) Match Separation and Creation

Figure 4: Graphical Representation of the Steady State

Notes. Panel 4a depicts the aggregate demand curve $c_d(p)$, the steady-state aggregate supply curve $c_s^{ss}(p)$, and the fixed productive capacity l. The lower price bound $p_{\min}$ is determined by Equation (22). Panel 4b illustrates the partial equilibrium in the upstream producer-retailer market, conditional on the steady-state price p^*. The loci $\mathbb{F}(\bar{z},\theta;p^*)=0$ and $\mathbb{H}(\bar{z},\theta)=0$ correspond to the match separation and match creation conditions, respectively, with the threshold $\bar{z}_{\min}$ defined by Equation (21). The steady-state values for consumption, price, the reservation transportation cost, and product market tightness are indicated by $c^*, p^*, \bar{z}^*$, and θ^*, respectively.

Panel 4b in Figure 4 provides the corresponding analysis for the upstream producer-retailer market in the $(\bar{z},\theta)$-plane. It illustrates the determination of the steady state through the intersection of the match separation condition (13) and the match creation condition (14).[12]

3.4. Comparative Statics

We examine the transmission of monetary policy shocks to macroeconomic aggregates, focusing on how the trade-off between price and output stabilization evolves during supply chain disruptions. Our tractable framework facilitates comparative statics that map the efficacy of monetary policy to the underlying state of the supply chain.

Monetary policy operates through changes in the nominal money supply, μ, while the severity of supply chain disruptions is governed by the scale parameter, γ, of the log-normal distribution of transportation costs. An increase in γ captures a general rise in transportation costs, consistent with Fact I. Proposition 3 formalizes how these supply chain disruptions alter the propagation of

[12]For further detail, Appendix E.3 in Bai et al. (2024) characterizes the geometry of these schedules. Under mild regularity conditions, the match separation locus $\mathbb{F}(\bar{z},\theta;p)=0$ implies a strictly decreasing and convex relationship between θ and $\bar{z}$, while the match creation locus $\mathbb{H}(\bar{z},\theta)=0$ describes a strictly increasing and convex relationship.

monetary policy shocks.

Proposition 3. *Consider the unique steady state characterized by the reservation transportation cost $\bar{z}^*$. Assume that (i) in the short run, the cutoff is invariant to supply chain disruptions (i.e., $d\bar{z}^*/d\gamma = 0$), and (ii) supply chain disruptions steepen the aggregate supply curve such that the sensitivities of the partial derivatives with respect to $\bar{z}$ satisfy the following inequality:*

$$\frac{\partial \ln S_{\bar{z}}}{\partial \gamma} < \frac{\partial \ln \Psi_{\bar{z}}}{\partial \gamma} < \frac{\partial \ln P_{\bar{z}}}{\partial \gamma}, \tag{23}$$

where $P(\bar{z})$ and $S(\bar{z})$ denote the implicit functions of $\bar{z}$ corresponding to the retail price p and matching share $S \equiv f(\theta)G(\bar{z})/\left(1 - G(\bar{z}) + f(\theta)G(\bar{z})\right)$, respectively, and $\Psi(\bar{z}) \equiv P(\bar{z})S(\bar{z})l$ denotes nominal aggregate supply.

Under these conditions, the baseline responses of the endogenous variables to a monetary policy shock are given by:

$$c_\mu > 0, \quad p_\mu > 0, \quad \kappa_\mu < 0, \quad \theta_\mu > 0, \quad r_\mu > 0, \quad \bar{z}_\mu > 0,$$

where $c, \kappa \equiv l - c, \theta$, and r denote consumption (equivalently, output), spare capacity, product market tightness, and wholesale price, respectively. Furthermore, the cross derivatives describing the state-dependent interaction between monetary policy and supply chain disruptions are:

$$c_{\mu\gamma} < 0, \quad p_{\mu\gamma} > 0, \quad \kappa_{\mu\gamma} > 0, \quad \theta_{\mu\gamma} \gtreqless 0, \quad r_{\mu\gamma} \gtreqless 0, \quad \bar{z}_{\mu\gamma} \gtreqless 0.$$

Proof. See Appendix A. ■

The partial and cross derivatives in Proposition 3 reveal that the state-dependent efficacy of monetary policy arises from the interaction of two distinct forces: the short-run rigidity of the reservation threshold (Condition (i)) and the steepening of the aggregate supply curve (Condition (ii)). The first condition acts as an anchor: because service contracts in containerized shipping prevent the reservation transportation cost $\bar{z}$ from adjusting immediately to supply chain disruptions ($d\bar{z}^*/d\gamma = 0$), the economy cannot re-optimize the set of viable matches.[13] This rigidity forces the adjustment to occur through the existing matches, where the second condition takes

[13] See Section 2.5 in Bai et al. (2024) for a detailed discussion of the short-run rigidities in containerized shipping. Specifically, the economic margin of frictions arises because service contracts typically fix invoiced freight rates for at least a one-month horizon. Consequently, the maximum transportation cost a match can bear without separation —the reservation transportation cost— remains rigid in the short run when underlying profitability does not change.

over: the distribution of rising transportation costs renders aggregate supply highly inelastic. Together, these conditions amplify the decline in retail prices while mitigating the drop in output caused by a contractionary monetary policy shock.[14]

Figure 5 provides a graphical representation of this theoretical prediction. In response to a contractionary monetary policy shock that reduces the nominal money supply μ, households decrease consumption due to reduced money holdings. This contractionary shock shifts the aggregate demand curve inward, from c_d (solid red line) to $c_{d,\mu\downarrow}$ (dash-dotted red line).

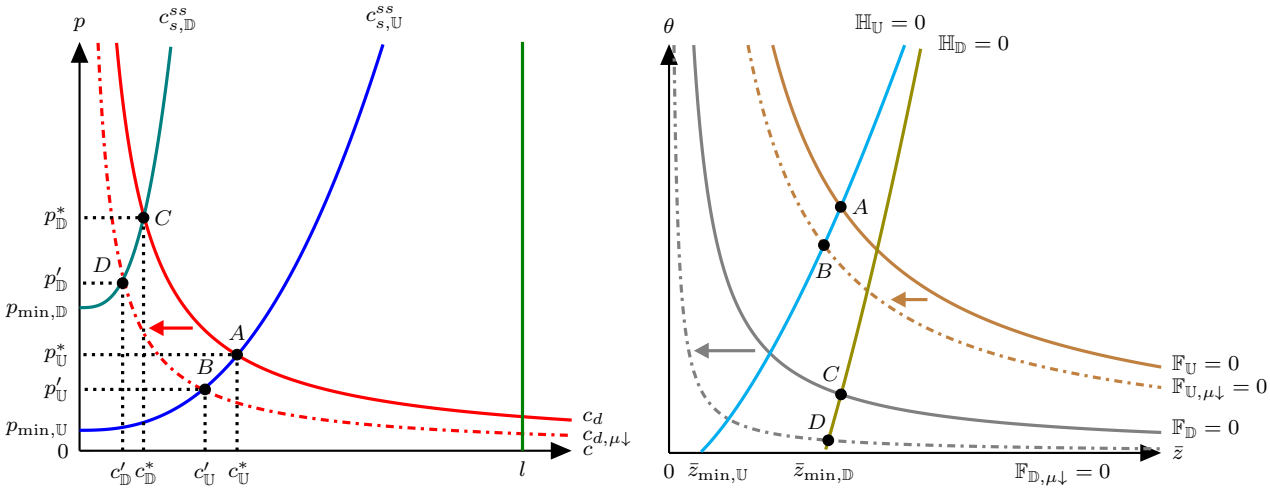

Figure 5: State-Dependent Effects of Monetary Contraction: Theoretical Predictions

Notes. The panels illustrate the economy's adjustment to a contractionary monetary policy shock, conditional on the underlying state of the supply chain. The subscripts $\mathbb{D}$ and $\mathbb{U}$ denote the disrupted and undisrupted states, respectively. In the left panel, c_d and $c_{d,\mu\downarrow}$ represent the aggregate demand curves before and after the shock, while $c^{ss}_{s,\mathbb{D}}$ and $c^{ss}_{s,\mathbb{U}}$ denote the aggregate supply curves. In the right panel, $\mathbb{F}_j = 0$ and $\mathbb{F}_{j,\mu\downarrow} = 0$ represent the match separation loci before and after the shock for state $j \in \{\mathbb{D}, \mathbb{U}\}$, while $\mathbb{H}_j = 0$ represents the corresponding match creation locus. Dash-dotted lines indicate the post-shock curves. The capital letters mark the transitions of the economy from A to B in the disrupted state and from C to D in the undisrupted state.

In the absence of supply chain disruptions, the aggregate supply curve is $c^{ss}_{s,\mathbb{U}}$ (solid blue line). The contractionary policy moves the economy's steady state from point A to B, resulting in a moderate price decrease and a notable output contraction. However, supply chain disruptions drastically alter this trade-off. The surge in transportation costs shifts the minimum price required to supply goods from $p_{\min,\mathbb{U}}$ to $p_{\min,\mathbb{D}}$ and, crucially, rotates the aggregate supply curve to $c^{ss}_{s,\mathbb{D}}$ (solid teal line). Consequently, the steady state shifts from point C to D.[15]

[14] The proposition also implies that the response of spare capacity is dampened during a supply chain disruption. Since spare capacity is defined as the residual of productive capacity minus actual production, the reduced sensitivity of output to monetary policy shocks directly translates to a reduced sensitivity of spare capacity.

[15] The right panel of Figure 5 illustrates the corresponding equilibrium dynamics in the upstream producer-

The geometric difference between these transitions ($A \to B$ vs. $C \to D$) is driven by the changing nature of the "marginal match" —the match that is just sufficiently profitable to survive at the reservation cost $\bar{z}$. We can interpret the sensitivity terms in Equation (23) as a divergence between the marginal volume contribution ($S_{\bar{z}}$) and the required price premium ($P_{\bar{z}}$).

In normal times (low γ), the distribution of transportation costs is well-behaved: extending the cutoff $\bar{z}$ allows many new matches to form (high marginal volume contribution) with only a modest increase in price (low required price premium). This generates a flatter aggregate supply curve ($c^{ss}_{s,\mathbb{U}}$). During a disruption ($\gamma \uparrow$), however, this relationship inverts. The cost shock effectively diminishes the density of viable matches at the margin. Consequently, supporting a marginal match requires a substantial price increase to cover the elevated transportation costs (high required price premium), yet this high-cost match contributes very little additional volume to the economy (low marginal volume contribution). This dynamic causes the aggregate supply curve to become steeper ($c^{ss}_{s,\mathbb{D}}$). Because the supply of goods is effectively "locked" by these cost constraints, a monetary contraction that tightens aggregate demand and moves the economy down this steep curve, achieving substantial price relief with a limited contraction in real output.

As an extension, Appendix B derives the theoretical prediction for monetary policy effectiveness when productive capacity l is constrained.[16] As with the scenario of supply chain disruptions, contractionary monetary policy proves more effective at stabilizing prices and reducing output sensitivity under constrained productive capacity.

3.5. Discussion

The stabilization trade-offs we derive are general features of economies with convex supply constraints. However, the source of this convexity is critical for identifying the underlying economic state. Our findings complement recent work by Benigno and Eggertsson (2023), who document the return of a non-linear *Phillips curve* during the post-pandemic recovery. While their framework attributes the convexity of the inflation-slack relationship to labor market shortages —where

retailer market in the $(\bar{z}, \theta)$-plane. A contractionary monetary policy shock shifts the match separation locus inward (from $\mathbb{F}_j = 0$ to $\mathbb{F}_{j,\mu\downarrow} = 0$ for $j \in \{\mathbb{D}, \mathbb{U}\}$), lowering both product market tightness and the reservation transportation cost.

[16] This extension is motivated by findings from our companion paper (Bai et al., 2024), which highlight that adverse shocks to productive capacity contributed to sustained U.S. inflation in 2022 due to the gradual increase in global oil prices, China's Omicron-related mobility restrictions, and labor market frictions in major U.S. trading partners.

a high vacancy-to-unemployment ratio drives up wage pressures— our model isolates the role of frictional goods markets and transportation bottlenecks in steepening the *aggregate supply curve*.

These two mechanisms operate at distinct stages of the supply chain. The labor channel (Benigno and Eggertsson, 2023) constrains the *production* of goods, whereas our transportation channel constrains the *distribution* of goods. Importantly, our mechanism demonstrates that the aggregate supply curve can steepen even if producers possess spare productive capacity (labor markets are not tight), provided that logistics and search frictions are sufficiently severe. This distinction highlights that supply chain bottlenecks can independently generate inflationary pressures and output rigidity, separate from labor market dynamics.

Furthermore, our results clarify that the micro-foundation of convexity matters for identifying the nature of supply constraints. Boehm and Pandalai-Nayar (2022), for instance, identify convexity arising from physical capacity constraints, where the supply curve steepens as plants approach their maximum utilization rates. In contrast, the convexity in our framework arises from rigidities in the transportation sector. Specifically, it is not governed solely by the curvature of the matching function ($f''(\theta) < 0$), but crucially by the interaction between rigid service contracts and the distribution of transportation costs ($G(z)$). In our model, supply chain disruptions (an increase in the scale parameter γ) drecrese the density of viable matches at the margin. This forces the economy onto the steep portion of the supply curve because the price premium required to support the marginal match rises disproportionately faster than the volume that match contributes to aggregate supply. Consequently, unlike physical capacity constraints which bind primarily at high output levels, supply chain disruptions can steepen the aggregate supply curve and inhibit monetary policy transmission even when physical output is below potential.

4. Empirical Evidence

Our theoretical framework implies that the transmission of monetary policy is state-dependent: contractionary shocks should yield stronger price effects and dampened output responses when the supply chain is disrupted. In this section, we examine whether U.S. data over the recent cycle aligns with these predictions using two complementary empirical approaches: a structural TVAR and LPs with interaction terms.

Our results must be interpreted with caution. Our sample spans from January 2017 to Septem-

ber 2023, a relatively short period that includes only one major episode of global supply chain disruptions. This episode coincided with the zero lower bound (ZLB), substantial fiscal stimulus, and unprecedented sectoral reallocation. Furthermore, the state of the supply chain is not purely exogenous; as noted by Gonçalves et al. (2024), state-dependent estimates can be sensitive when the state variable is persistent or endogenous to the shock itself —for instance, loose monetary policy likely contributed to demand that exacerbated port congestion. Given these constraints, we view the following analysis not as a definitive causality assessment, but as descriptive evidence that the macroeconomic data are consistent with the mechanisms highlighted in our theoretical model.

4.1. A TVAR Model

To examine our theoretical predictions, we estimate a structural TVAR model following Chen and Lee (1995) that allows for regime-dependent parameter variations to capture non-linear dynamics:

$$\boldsymbol{y}_t = I_t \left[\sum_{l=1}^{L} \boldsymbol{B}'_{\mathbb{D},l} \boldsymbol{y}_{t-l} + \boldsymbol{C}'_{\mathbb{D}} \boldsymbol{\omega}_t + \boldsymbol{\Sigma}_{\mathbb{D}}^{1/2} \boldsymbol{\epsilon}_t \right] + (1 - I_t) \left[\sum_{l=1}^{L} \boldsymbol{B}'_{\mathbb{U},l} \boldsymbol{y}_{t-l} + \boldsymbol{C}'_{\mathbb{U}} \boldsymbol{\omega}_t + \boldsymbol{\Sigma}_{\mathbb{U}}^{1/2} \boldsymbol{\epsilon}_t \right], \tag{24}$$

where $\boldsymbol{y}_t$ is an $n \times 1$ vector of endogenous variables and $\boldsymbol{\omega}_t = [1, t]'$ accounts for deterministic constant and trend terms. The structural shocks $\boldsymbol{\epsilon}_t$ are assumed to be Gaussian with $\boldsymbol{\epsilon}_t \sim \mathcal{N}(\mathbf{0}, \mathbf{1}_{n \times n})$. The subscripts $\mathbb{D}$ and $\mathbb{U}$ denote the disrupted and undisrupted supply chain states, respectively. In our baseline specification, we set the lag length to $L = 1$.

Regime switching is governed by the indicator variable $I_t \in \{0, 1\}$. We determine the threshold separating these states using the ACR index (Bai et al., 2023, 2024). Derived from satellite-based AIS data via a density-based spatial clustering algorithm, the ACR index serves as a real-time proxy for the operational state of global supply chains. The indicator I_t triggers the disrupted regime if the lagged index, ACR_{t-1}, exceeds the estimated threshold $\overline{\text{ACR}}$:

$$I_t = \begin{cases} 1, & \text{if } \text{ACR}_{t-1} > \overline{\text{ACR}}; \\ 0, & \text{if } \text{ACR}_{t-1} \leq \overline{\text{ACR}}. \end{cases}$$

Consistent with our theoretical framework, the endogenous vector $\boldsymbol{y}_t$ comprises monthly U.S. data on real GDP, the PCE goods price index, the import price index, and our constructed measures of product market tightness and spare capacity. We also include the ACR index and

the federal funds rate, the latter capturing the stance of U.S. monetary policy. Real GDP, the PCE goods price, product market tightness, and the import price enter the model in log percent, while the federal funds rate, the spare capacity rate, and the ACR index enter in levels.[17]

While Section 2 defines the measure of product market tightness, we construct the empirical measure of spare capacity to match its theoretical counterpart. Specifically, we calculate the average spare capacity rate for the top five U.S. trading partners —Mexico, Canada, China, Germany, and Japan—weighted by their shares of U.S. goods imports:

$$\text{SpareCapacityRate}_t = \sum_{i \in \mathscr{C}} \left[\frac{\text{Import}_{i,t}}{\sum_{j \in \mathscr{C}} \text{Import}_{j,t}} \cdot \left(100 - \text{CapacityUtilization}_{i,t}\right) \right],$$

where $\mathscr{C}$ denotes the set of trading partners. Additionally, we use the import price index as a proxy for the wholesale price to capture the international sourcing strategies of U.S. firms.

To identify a contractionary monetary policy shock, we follow the theoretical predictions in Proposition 3 and impose the following restrictions on the impulse response functions (IRFs):

Restriction 1. *A contractionary monetary policy shock results in a negative impact response of real GDP, the PCE goods price, product market tightness, and the import price, along with a positive impact response of the spare capacity rate and the federal funds rate. The ACR index does not respond on impact.*

This zero restriction reflects the short-run insensitivity of global port congestion to U.S. monetary policy at a monthly frequency. Because containerized shipments involve long-term contracts and transportation times that often extend beyond a month, the ACR index remains largely unaffected by contemporaneous policy shocks.[18]

We estimate the model and the identified set of IRFs using a Bayesian approach (Mumtaz and Zanetti, 2015; Pizzinelli et al., 2020; Bratsiotis and Theodoridis, 2022).[19] To implement the sign and zero restrictions, we adopt the penalty function approach (PFA) developed by Uhlig (2005)

[17] Data sources are detailed in Appendix C. Except for the federal funds rate, all series are seasonally adjusted.

[18] As discussed in Bai et al. (2024), liner shipping companies adjust "tactical-level" decisions —such as shipping frequency, capacity deployment, and cruising speed— only every three to six months in response to demand shifts (Stopford, 2008; Meng et al., 2014). Furthermore, we formally test this assumption in Bai et al. (2024) and find no significant contemporaneous response of the ACR index to a Bauer-Swanson monetary policy shock (Bauer and Swanson, 2023).

[19] Under a Normal-Inverse-Wishart conjugate prior for the TVAR parameters and conditional on the threshold value $\overline{\text{ACR}}$, the posterior distribution follows a conditional Normal-Inverse-Wishart distribution. We use the Gibbs sampler to draw from this distribution and a Metropolis-Hastings algorithm to estimate the posterior of $\overline{\text{ACR}}$ following Chen and Lee (1995) and Pizzinelli et al. (2020). Further details are in Appendix E.1.

and Mountford and Uhlig (2009). This method employs a loss function to identify an impulse vector that satisfies the zero restrictions, and either meets or approximates the sign restrictions (see Appendix E.2 for details).

Figure 6 presents the IRFs to a contractionary monetary policy shock for the supply chain disrupted (black) and undisrupted (red) regimes, showing both the point-wise posterior medians (solid lines) and the 68% equal-tailed credible intervals (shaded areas and dotted lines) from horizon $k = 0$ to $k = 12$. Appendix E.3 presents the posterior distribution of $\overline{\text{ACR}}$ and the resulting time series of identified regimes.

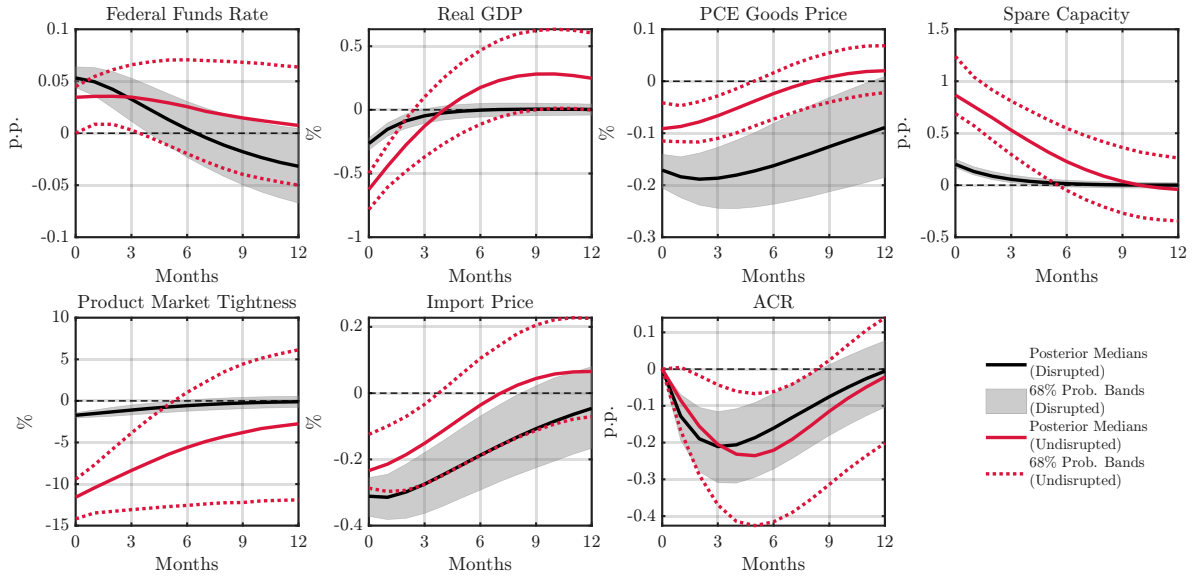

Figure 6: State-Dependent Effects of Monetary Contraction: Empirical Evidence From TVAR

Notes. IRFs to a one-standard-deviation contractionary monetary policy shock, identified using Restriction 1, for supply chain disrupted and undisrupted regimes. Solid black (red) lines represent point-wise posterior medians, while the shaded black area (dotted red lines) depicts 68% equal-tailed credible intervals for the disrupted (undisrupted) regime. Estimates are based on 10,000 independent draws from the posterior of a Bayesian structural TVAR.

The figure reveals differences in the responses of the endogenous variables across the two regimes. Consistent with the theoretical predictions of Proposition 3, PCE goods prices are notably more responsive, whereas real GDP and the spare capacity rate exhibit less responsiveness in the disrupted regime; these differences are well-supported by the posterior probability distribution.[20] Such a divergence reinforces the notion that the economy operates on a steeper aggregate supply curve during periods of supply chain disruption.

[20] We also find that, despite the lack of formal theoretical predictions, product market tightness is less responsive while import prices are more responsive to monetary contraction in the disrupted state. The response of the ACR index, however, cannot be clearly differentiated across the posterior distribution.

The responses of the federal funds rate align with these patterns: in the undisrupted regime, the rate remains elevated for most horizons, while it dips below the baseline after two quarters in the disrupted regime.

Appendix F demonstrates that our findings are robust to several variations of the baseline model: (i) replacing the ACR index with the index of Average Congestion Time (ACT) to proxy for supply chain states; (ii) incorporating the Wu-Xia shadow federal funds rate (Wu and Xia, 2016); (iii) using an alternative measure of product market tightness defined as the ratio of U.S. retailers' new orders to the import-weighted average spare capacity; (iv) relaxing the zero restriction on the ACR index at horizon $k = 0$; (v) applying alternative lag structures; (vi) adopting a looser prior ($\lambda = 0.5$); and (vii) including only a constant in the TVAR specification.

4.2. An LP Model

Next, we employ LPs to identify a contractionary monetary policy shock conditional on the state of the global supply chain. LPs provide a flexible framework for capturing state-dependent effects without imposing strong parametric assumptions. However, we acknowledge that state-dependent LPs may be biased when the state variable is highly persistent, as is the case for our ACR index. We therefore treat the next results as complementary to our TVAR findings rather than definitive.

Following Ramey and Zubairy (2018), Ghassibe and Zanetti (2022), and Arias et al. (2023), we use LPs with interaction terms, with identification based on sign restrictions implemented following Plagborg-Møller and Wolf (2021). Consider the $n \times (K+1)$ projections:

$$\begin{aligned} y_{i,t+k} =& I_{t-1}\left[\boldsymbol{\beta}'_{\mathbb{D},i,k,0}\boldsymbol{y}_t + \sum_{l=1}^{L}\boldsymbol{\beta}'_{\mathbb{D},i,k,l}\boldsymbol{y}_{t-l} + \boldsymbol{C}'_{\mathbb{D},i,k}\boldsymbol{\omega}_t\right] \\ &+ (1-I_{t-1})\left[\boldsymbol{\beta}'_{\mathbb{U},i,k,0}\boldsymbol{y}_t + \sum_{l=1}^{L}\boldsymbol{\beta}'_{\mathbb{U},i,k,l}\boldsymbol{y}_{t-l} + \boldsymbol{C}'_{\mathbb{U},i,k}\boldsymbol{\omega}_t\right] + u_{i,k,t}, \end{aligned}$$

where $y_{i,t+k}$ is the value of the i-th variable in $\boldsymbol{y}_{t+k}$, and $\boldsymbol{y}_t$ is an $n \times 1$ vector of the same endogenous variables used in the TVAR (excluding the ACR index itself). The vector $\boldsymbol{\omega}_t = [1, t]'$ contains a constant and a linear trend, while $u_{i,k,t}$ denotes the k-step-ahead forecast error. The vector of the error terms at $k = 1$, $\boldsymbol{u}_{1,t} = [u_{1,1,t}, \ldots, u_{n,1,t}]'$, is assumed to have mean zero and variance-covariance matrix $\mathbb{E}(\boldsymbol{u}_{1,t}\boldsymbol{u}'_{1,t}) = \boldsymbol{\Sigma}$. Consistent with our TVAR specification, we use a single lag ($L = 1$) to minimize parameter uncertainty.

I_{t-1} is an indicator variable for the supply chain state. Here, the disrupted regime is defined as periods during which the ACR index at time $t-1$ exceeds its sample median. Figure 7 plots the ACR index alongside this median threshold. Prior to mid-2017, the index consistently remained above its median, indicating a disrupted state. This pattern shifted from late 2017 through 2020, during which the index remained below the median, before reversing again in early 2021 as the global economy re-entered the disrupted regime.[21]

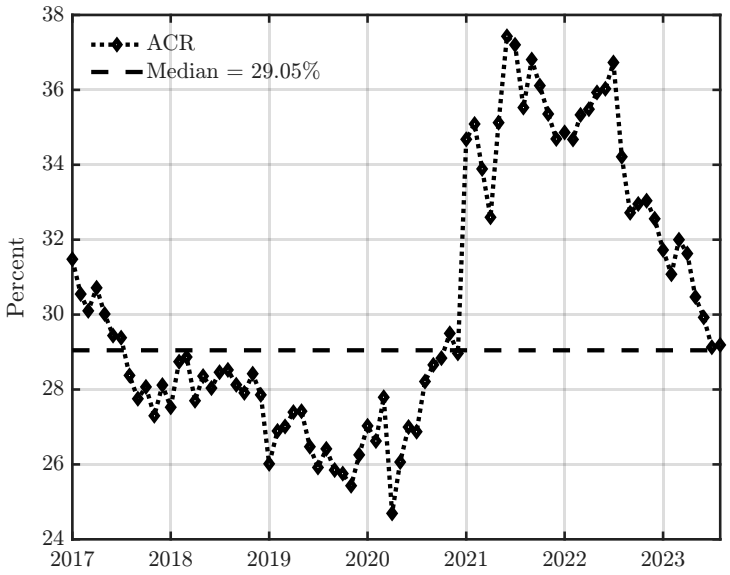

Figure 7: ACR and Sample Median

Notes. The figure plots the ACR index and its sample median from January 2017 to August 2023.

To identify a contractionary monetary policy shock, we follow the theoretical predictions of Proposition 3 and adopt an identification scheme analogous to that used in the TVAR approach. However, because the ACR index is not included as an endogenous variable, we omit the zero restriction and instead impose the following sign and elasticity restrictions:

Restriction 1′. *A contractionary monetary policy shock induces negative responses in real GDP, the PCE goods price index, product market tightness, and the import price index, alongside positive responses in the federal funds rate and the spare capacity rate at horizons* $k = 0, 1, 2$. *Furthermore, the magnitude of the impact response of real GDP (in percent) is bounded above by 10 times the magnitude of the impact response of the federal funds rate (in percentage points).*

[21] Notably, the regime transitions in Figure 7 closely align with those in Figure E.1, where the threshold $\overline{\text{ACR}}$ is endogenously determined by the TVAR estimation.

Restriction 1′ extends the sign restrictions beyond the impact horizon to sharpen identification and introduces an elasticity bound to ensure the plausibility of the identified set.[22]

We determine the identified set for each regime by numerically solving the quadratic program from the supplement to Plagborg-Møller and Wolf (2021) using Algorithm 2 in Giacomini and Kitagawa (2021). Let $\boldsymbol{S}_1$ denote a $12 \times n$ matrix that selects the IRFs restricted to be negative, and let $\boldsymbol{S}_2$ denote a $6 \times n$ matrix that selects the IRFs restricted to be positive (for a total of 18 sign restrictions in Restriction 1′). For each regime $r \in \{\mathbb{D}, \mathbb{U}\}$, we draw $D = 100,000$ orthogonal matrices $\boldsymbol{Q}_{r,d}$ satisfying:

$$\boldsymbol{S}_1 \hat{\boldsymbol{B}}_{r,0:2} \hat{\boldsymbol{\Omega}} \boldsymbol{Q}_{r,d} \boldsymbol{e}_1 \leq 0, \quad \boldsymbol{S}_2 \hat{\boldsymbol{B}}_{r,0:2} \hat{\boldsymbol{\Omega}} \boldsymbol{Q}_{r,d} \boldsymbol{e}_1 \geq 0, \quad \frac{\boldsymbol{e}_2' \hat{\boldsymbol{B}}_{r,0} \hat{\boldsymbol{\Omega}} \boldsymbol{Q}_{r,d} \boldsymbol{e}_1}{\boldsymbol{e}_1' \hat{\boldsymbol{B}}_{r,0} \hat{\boldsymbol{\Omega}} \boldsymbol{Q}_{r,d} \boldsymbol{e}_1} \geq -10, \tag{25}$$

where $1 \leq d \leq D$, $\hat{\boldsymbol{B}}_{r,0:2} = [\hat{\boldsymbol{B}}_{r,0}' \ \hat{\boldsymbol{B}}_{r,1}' \ \hat{\boldsymbol{B}}_{r,2}']'$, $\hat{\boldsymbol{B}}_{r,k} = [\hat{\boldsymbol{\beta}}_{r,1,k,0} \ \dots \ \hat{\boldsymbol{\beta}}_{r,n,k,0}]'$, $\hat{\boldsymbol{\beta}}_{r,i,k,0}$ is the OLS estimate of $\boldsymbol{\beta}_{r,i,k,0}$, $\hat{\boldsymbol{\Omega}} = \text{chol}(\hat{\boldsymbol{\Sigma}})'$, chol is the upper triangular Cholesky decomposition, $\hat{\boldsymbol{\Sigma}}$ is the OLS estimate of $\boldsymbol{\Sigma}$, and $\boldsymbol{e}_i$ is the i-th column of the n-dimensional identity matrix. The first two conditions in Equation (25) summarize the sign restrictions, while the third condition imposes the elasticity bound. The identified set of IRFs for the i-th variable at horizon k is given by:

$$\left[\min_d \left\{ 0.05 \frac{\boldsymbol{e}_i' \hat{\boldsymbol{B}}_{r,k} \hat{\boldsymbol{\Omega}} \boldsymbol{Q}_{r,d} \boldsymbol{e}_1}{\boldsymbol{e}_1' \hat{\boldsymbol{B}}_{r,0} \hat{\boldsymbol{\Omega}} \boldsymbol{Q}_{r,d} \boldsymbol{e}_1} \right\}, \ \max_d \left\{ 0.05 \frac{\boldsymbol{e}_i' \hat{\boldsymbol{B}}_{r,k} \hat{\boldsymbol{\Omega}} \boldsymbol{Q}_{r,d} \boldsymbol{e}_1}{\boldsymbol{e}_1' \hat{\boldsymbol{B}}_{r,0} \hat{\boldsymbol{\Omega}} \boldsymbol{Q}_{r,d} \boldsymbol{e}_1} \right\} \right],$$

where the factor $0.05/(\boldsymbol{e}_1' \hat{\boldsymbol{B}}_{r,0} \hat{\boldsymbol{\Omega}} \boldsymbol{Q}_{r,d} \boldsymbol{e}_1)$ normalizes the contractionary monetary policy shock to a 5-basis-point increase in the federal funds rate on impact.

Figure 8 presents the estimated identified sets for the IRFs across both regimes. Consistent with the TVAR results in Figure 6, the LP estimates reveal similar state-dependent dynamics over a six-month horizon ($k = 0$ to $k = 6$).[23] In the disrupted regime, a contractionary monetary policy shock generates muted responses in real GDP and spare capacity relative to the undisrupted regime, but a substantially stronger decline in PCE goods prices, especially in the short run following impact.

In summary, although the limited sample size and the presence of concurrent shocks warrant caution, both empirical methodologies yield consistent conclusions. During periods of supply chain disruption, the aggregate supply curve steepens, granting monetary policy greater traction

[22] Following Kilian and Murphy (2012) and Arias et al. (2023), this bound rules out extreme IRFs in which a small policy move triggers an implausibly large decline in real GDP.

[23] The shorter horizon relative to that of the IRFs shown in the TVAR is due to the length of our sample and the parameter uncertainty associated with LPs.

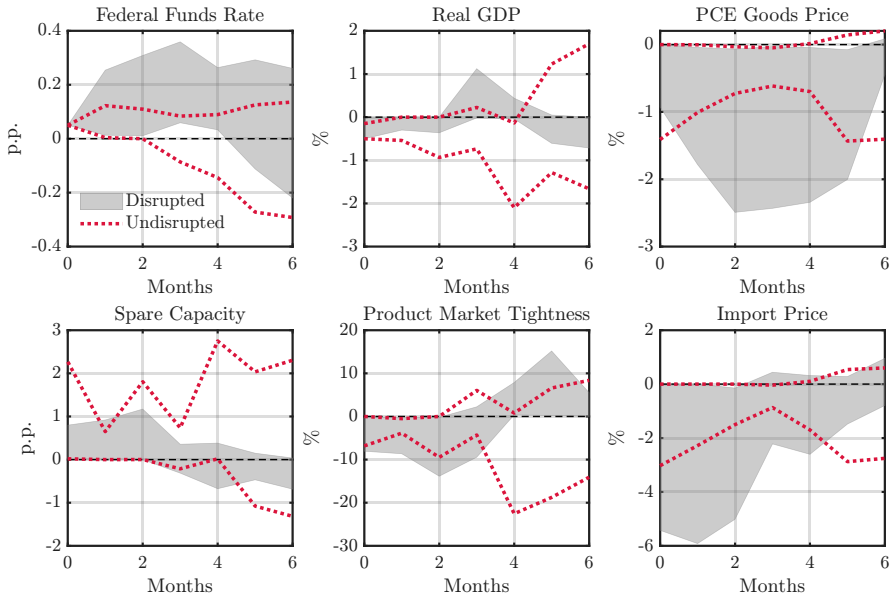

Figure 8: State-Dependent Effects of Monetary Contraction: Empirical Evidence From LP

Notes. IRFs to a contractionary monetary policy shock identified using Restriction 1′, estimated via LPs with interaction terms. The regimes are defined using the sample median of the ACR index as a threshold. The shaded areas (for the disrupted regime) and the dotted lines (for the undisrupted regime) depict the estimated identified sets. Results are based on 100,000 orthogonal matrix draws.

over prices at the expense of its impact on real output.

5. Conclusion

Our analysis examines the efficacy of contractionary monetary policy in controlling price increases during global supply chain disruptions. Motivated by stylized facts linking logistical bottlenecks, transportation costs, and the co-movement of product market tightness and goods prices, we develop a tractable framework in which frictional trade between producers and retailers, together with transportation costs, generates a convex aggregate supply curve. A key insight of our model is that supply chain disturbances do not merely constrain the level of output but steepen the supply schedule. This heightened convexity amplifies the responsiveness of prices to demand adjustments while rendering output relatively inelastic. We find that the data are consistent with this mechanism: estimates from both structural TVAR and LP models suggest that during periods of supply chain disruption, monetary contraction is associated with a significantly stronger decline in goods prices relative to the output cost. These findings support the view that the trade-off between price and output stabilization improves when logistical frictions constrain the economy.

Our study opens several promising avenues for future research. First, while we focus on monetary policy, the convexity of the supply curve has equally profound implications for fiscal policy. Future work could investigate how the fiscal multiplier varies with the state of supply chains; our framework suggests that fiscal stimulus during logistical disruptions may be particularly inflationary with limited output gains, a hypothesis that warrants formal testing. Second, our model takes the supply chain structure as given. A valuable extension would be to endogenize the formation of trading relationships in a dynamic setting.[24] Understanding how stabilization policy interacts with firms' long-term decisions to diversify suppliers or re-shore production —potentially altering the slope of the supply curve endogenously— would connect business cycle stabilization with structural trade dynamics. Third, our analysis abstracts from sectoral heterogeneity. Given that supply chain bottlenecks often originate in specific industries before propagating, extending our framework to a multi-sector production network could uncover how monetary policy transmission differs when "convexity" is concentrated in upstream versus downstream sectors. We plan to pursue some of these extensions in future work.

References

Alpanda, S., Granziera, E., and Zubairy, S. (2021). State Dependence of Monetary Policy Across Business, Credit and Interest Rate Cycles. *European Economic Review*, 140:103936.

Angrist, J. D., Jorda, O., and Kuersteiner, G. M. (2018). Semiparametric Estimates of Monetary Policy Effects: String Theory Revisited. *Journal of Business & Economic Statistics*, 36(3):371–387.

Arias, J. E., Fernández-Villaverde, J., Rubio-Ramírez, J. F., and Shin, M. (2023). The Causal Effects of Lockdown Policies on Health and Macroeconomic Outcomes. *American Economic Journal: Macroeconomics*, 15(3):287–319.

Bai, X., Fernández-Villaverde, J., Li, Y., Marto, R., and Zanetti, F. (2025). Shipping to America. Working paper, University of Oxford.

Bai, X., Fernández-Villaverde, J., Li, Y., and Zanetti, F. (2024). The Causal Effects of Global Supply Chain Disruptions on Macroeconomic Outcomes: Evidence and Theory. Working Paper 32098, National Bureau of Economic Research.

Bai, X., Ma, Z., Hou, Y., Li, Y., and Yang, D. (2023). A Data-Driven Iterative Multi-Attribute Clustering Algorithm and Its Application in Port Congestion Estimation. *IEEE Transactions on Intelligent Transportation Systems*, 24:12026–12037.

[24] See Xu et al. (2025) for a model with endogenous adoption and termination of suppliers over business cycles.

Balleer, A. and Noeller, M. (2023). Monetary Policy in the Presence of Supply Constraints: Evidence From German Firm-Level Data. Working Paper 10261, CESifo.

Bauer, M. D. and Swanson, E. T. (2023). A Reassessment of Monetary Policy Surprises and High-Frequency Identification. *NBER Macroeconomics Annual*, 37:87–155.

Benigno, P. and Eggertsson, G. B. (2023). It's Baaack: The Surge in Inflation in the 2020s and the Return of the Non-Linear Phillips Curve. Working Paper 31197, National Bureau of Economic Research.

Benigno, P. and Ricci, L. A. (2011). The Inflation-Output Trade-off With Downward Wage Rigidities. *American Economic Review*, 101(4):1436–66.

Berger, D., Milbradt, K., Tourre, F., and Vavra, J. (2021). Mortgage Prepayment and Path-Dependent Effects of Monetary Policy. *American Economic Review*, 111(9):2829–78.

Bernanke, B. and Blanchard, O. (2025). What Caused the US Pandemic-Era Inflation? *American Economic Journal: Macroeconomics*, 17(3):1–35.

Bernstein, J. (2021). A Model of State-Dependent Monetary Policy. *Journal of Monetary Economics*, 117:904–917.

Bilbiie, F. O., Primiceri, G., and Tambalotti, A. (2023). Inequality and Business Cycles. Working Paper 31729, National Bureau of Economic Research.

Boehm, C. E. and Pandalai-Nayar, N. (2022). Convex Supply Curves. *American Economic Review*, 112(12):3941–69.

Bratsiotis, G. J. and Theodoridis, K. (2022). Precautionary Liquidity Shocks, Excess Reserves and Business Cycles. *Journal of International Financial Markets, Institutions and Money*, 77:101518.

Chen, C. W. and Lee, J. C. (1995). Bayesian Inference of Threshold Autoregressive Models. *Journal of Time Series Analysis*, 16:483–492.

Comín, D. A., Johnson, R. C., and Jones, C. J. (2023). Supply Chain Constraints and Inflation. Working Paper 31179, National Bureau of Economic Research.

di Giovanni, J., Şebnem Kalemli-Özcan, Silva, A., and Yildirim, M. A. (2022). Global Supply Chain Pressures, International Trade, and Inflation. Working Paper 30240, National Bureau of Economic Research.

di Giovanni, J., Şebnem Kalemli-Özcan, Silva, A., and Yildirim, M. A. (2023). Pandemic-Era Inflation Drivers and Global Spillovers. Working Paper 31887, National Bureau of Economic Research.

Eichenbaum, M., Rebelo, S., and Wong, A. (2022). State-Dependent Effects of Monetary Policy: The Refinancing Channel. *American Economic Review*, 112(3):721–61.

Eichenbaum, M. S., Puglisi, F., Rebelo, S., and Trabandt, M. (2025). Banks and the State-Dependent Effects of Monetary Policy. Working Paper 33523, National Bureau of Economic Research.

Ferrante, F., Graves, S., and Iacoviello, M. (2023). The Inflationary Effects of Sectoral Reallocation. *Journal of Monetary Economics*, 140:S64–S81.

Gagliardone, L. and Gertler, M. (2023). Oil Prices, Monetary Policy and Inflation Surges. Working Paper 31263, National Bureau of Economic Research.

Ganapati, S., Wong, W. F., and Ziv, O. (2024). Entrepôt: Hubs, Scale, and Trade Costs. *American Economic Journal: Macroeconomics*, 16(4):239–78.

Ghassibe, M. and Zanetti, F. (2022). State Dependence of Fiscal Multipliers: The Source of Fluctuations Matters. *Journal of Monetary Economics*, 132:1–23.

Giacomini, R. and Kitagawa, T. (2021). Robust Bayesian Inference for Set-Identified Models. *Econometrica*, 89:1519–1556.

Giannone, D. and Primiceri, G. (2024). The Drivers of Post-Pandemic Inflation. Working Paper 32859, National Bureau of Economic Research.

Gonçalves, S., Herrera, A. M., Kilian, L., and Pesavento, E. (2024). State-Dependent Local Projections. *Journal of Econometrics*, 244(2):105702.

Guerrieri, V., Lorenzoni, G., Straub, L., and Werning, I. (2022). Macroeconomic Implications of COVID-19: Can Negative Supply Shocks Cause Demand Shortages? *American Economic Review*, 112(5):1437–74.

Harding, M. and Klein, M. (2022). Monetary Policy and Household Net Worth. *Review of Economic Dynamics*, 44:125–151.

Harding, M., Lindé, J., and Trabandt, M. (2023). Understanding Post-COVID Inflation Dynamics. *Journal of Monetary Economics*.

Ikeda, D., Li, S., Mavroeidis, S., and Zanetti, F. (2024). Testing the Effectiveness of Unconventional Monetary Policy in Japan and the United States. *American Economic Journal: Macroeconomics*, 16(2):250–86.

Keynes, J. M. (1940). How to Pay for the War. In *Essays in Persuasion*, pages 367–439. Springer.

Kilian, L. and Murphy, D. P. (2012). Why Agnostic Sign Restrictions Are Not Enough: Understanding the Dynamics of Oil Market VAR Models. *Journal of the European Economic Association*, 10:1166–1188.

Lippi, F., Ragni, S., and Trachter, N. (2015). Optimal Monetary Policy With Heterogeneous Money Holdings. *Journal of Economic Theory*, 159:339–368.

Liu, P., Theodoridis, K., Mumtaz, H., and Zanetti, F. (2019). Changing Macroeconomic Dynamics at the Zero Lower Bound. *Journal of Business & Economic Statistics*, 37(3):391–404.

Meng, Q., Wang, S., Andersson, H., and Thun, K. (2014). Containership Routing and Scheduling in Liner Shipping: Overview and Future Research Directions. *Transportation Science*, 48(2):265–280.

Michaillat, P. and Saez, E. (2015). Aggregate Demand, Idle Time, and Unemployment. *Quarterly Journal of Economics*, 130:507–569.

Michaillat, P. and Saez, E. (2022). An Economical Business-Cycle Model. *Oxford Economic Papers*, 74:382–411.

Miyamoto, W., Nguyen, T., and Sergeyev, D. (2024). How Oil Shocks Propagate: Evidence on the Monetary Policy Channel. Working Paper 2024-07, Federal Reserve Bank of San Francisco.

Mountford, A. and Uhlig, H. (2009). What Are the Effects of Fiscal Policy Shocks? *Journal of Applied Econometrics*, 24:960–992.

Mumtaz, H. and Zanetti, F. (2015). Labor market dynamics: A time-varying analysis. *Oxford Bulletin of Economics and Statistics*, 77(3):319–338.

Pizzinelli, C., Theodoridis, K., and Zanetti, F. (2020). State Dependence in Labor Market Fluctuations. *International Economic Review*, 61:1027–1072.

Plagborg-Møller, M. and Wolf, C. K. (2021). Local Projections and VARs Estimate the Same Impulse Responses. *Econometrica*, 89:955–980.

Ramey, V. A. and Zubairy, S. (2018). Government Spending Multipliers in Good Times and in Bad: Evidence From US Historical Data. *Journal of Political Economy*, 126:850–901.

Stock, J. H. and Watson, M. W. (2025). Recovering From COVID. Working Paper 33857, National Bureau of Economic Research.

Stopford, M. (2008). *Maritime Economics*. Routledge, London, 3 edition.

Tenreyro, S. and Thwaites, G. (2016). Pushing on a String: US Monetary Policy Is Less Powerful in Recessions. *American Economic Journal: Macroeconomics*, 8(4):43–74.

Uhlig, H. (2005). What Are the Effects of Monetary Policy on Output? Results From an Agnostic Identification Procedure. *Journal of Monetary Economics*, 52:381–419.

UNCTAD (2022). Review of Maritime Transport 2022. UNCTAD.

Verduzco-Bustos, G. and Zanetti, F. (2026). The effects of geopolitical oil price shocks. Working paper, University of Oxford.

Wu, J. C. and Xia, F. D. (2016). Measuring the Macroeconomic Impact of Monetary Policy at the Zero Lower Bound. *Journal of Money, Credit and Banking*, 48(2-3):253–291.

Xu, L., Yu, Y., and Zanetti, F. (2025). The Adoption and Termination of Suppliers Over the Business Cycle. *Journal of Monetary Economics*, 151:103730.

Online Appendices

State Dependence of Monetary Policy During Global Supply Chain Disruptions

Xiwen Bai[†], *Jesús Fernández-Villaverde*[‡], *Yiliang Li*[§], *Francesco Zanetti*[¶]

Contents

† Bai: Tsinghua University, China. xiwenbai@mail.tsinghua.edu.cn. ‡ Fernández-Villaverde: University of Pennsylvania, U.S. jesusfv@econ.upenn.edu. § Li: University of International Business and Economics, China. yiliang_li@uibe.edu.cn. ¶ Zanetti: University of Oxford, U.K. francesco.zanetti@economics.ox.ac.uk.

A. Proof of Proposition 3

The proof proceeds in three steps: first, we reduce the three-equation system —the match separation condition $\mathbb{F}(p, \bar{z}, \theta) = 0$, match creation condition $\mathbb{H}(\bar{z}, \theta) = 0$, and retailer-household market clearing condition $c_s^{ss}(\bar{z}, \theta) = c_d(p)$— to a single equation in terms of the reservation transportation cost $\bar{z}$ by establishing the properties of the implicit functions for tightness, retail price, and matching share; second, we derive the comparative statics with respect to a monetary policy shock μ; and third, we analyze the cross derivatives with respect to the supply chain parameter γ to establish the state-dependent responses.

A.1. System Reduction and Existence

We express the endogenous variables as implicit functions of $\bar{z}$. Define $I(\bar{z}) \equiv \int_0^{\bar{z}} G(z')dz'$.

Tightness. Using the match creation condition $\mathbb{H}(\bar{z}, \theta) = 0$, product market tightness is implicitly defined by:

$$\frac{\rho}{q(\theta)} = (1 - \eta)\beta I(\bar{z}). \tag{A.1}$$

Differentiating with respect to $\bar{z}$ yields:

$$-\frac{\rho q'(\theta)}{q(\theta)^2}\frac{\partial \theta}{\partial \bar{z}} = (1 - \eta)\beta G(\bar{z}) \implies \Theta_{\bar{z}} = \frac{(1 - \eta)\beta G(\bar{z}) q(\theta)^2}{-\rho q'(\theta)}.$$

Since $q'(\theta) < 0$ and $G(\bar{z}) > 0$, it follows that $\Theta_{\bar{z}} > 0$.

Retail price. Substituting $\Theta(\bar{z})$ into the match separation condition $\mathbb{F}(p, \bar{z}, \theta) = 0$ yields the retail price function:

$$P(\bar{z}) = \bar{z} - \left[1 - \eta f\left(\Theta(\bar{z})\right)\right] \beta I(\bar{z}). \tag{A.2}$$

Differentiating with respect to $\bar{z}$:

$$P_{\bar{z}} = \underbrace{1 - \left(1 - \eta f(\theta)\right) \beta G(\bar{z})}_{>0} + \underbrace{\eta \beta I(\bar{z}) f'(\theta) \Theta_{\bar{z}}}_{>0}.$$

The first term is positive because $\beta < 1$, $G(\bar{z}) < 1$, and $(1 - \eta f(\theta)) < 1$. The second is positive because $f'(\theta) > 0$ and $\Theta_{\bar{z}} > 0$. Thus, $P_{\bar{z}} > 0$.

Matching share. Substituting $\Theta(\bar{z})$ into the definition of matching share S yields:

$$S(\bar{z}) = \frac{f\left(\Theta(\bar{z})\right) G(\bar{z})}{1 - G(\bar{z}) + f\left(\Theta(\bar{z})\right) G(\bar{z})}. \tag{A.3}$$

To verify the sign of $S_{\bar{z}}$, we rearrange the expression:

$$S(\bar{z}) = \left[1 + \frac{1 - G(\bar{z})}{f\left(\Theta(\bar{z})\right) G(\bar{z})}\right]^{-1}.$$

Since both $G(\bar{z})$ and $f\left(\Theta(\bar{z})\right)$ are strictly increasing in $\bar{z}$, the term in the bracket decreases, implying $S_{\bar{z}} > 0$.

Nominal aggregate supply. Recall that the nominal aggregate supply is defined as $\Psi(\bar{z}, \gamma) \equiv P(\bar{z})S(\bar{z})l$. Differentiating with respect to $\bar{z}$ yields:

$$\Psi_{\bar{z}} = (P_{\bar{z}}S + PS_{\bar{z}})l > 0.$$

Meanwhile, as established in Proposition 2, the lower bound of $\bar{z}$ satisfies $(1-\eta)\beta I(\bar{z}_{\min}) = \rho$.[1] As $\bar{z} \to \bar{z}_{\min}^{+}$, $\theta \to 0$, hence $S \to 0$ and $\Psi \to 0$. On the other hand, as $\bar{z} \to +\infty$, $P \to +\infty$ and hence, $\Psi \to +\infty$. By the Intermediate Value Theorem, there exists a unique $\bar{z}^*$ satisfying the market clearing condition $\Psi(\bar{z}^*) = \chi^{\varepsilon}\mu$.

A.2. Comparative Statics

Total differentiation of the market clearing condition $\Psi(\bar{z}^*) = \chi^{\varepsilon}\mu$ with respect to μ yields:

$$\bar{z}_{\mu} = \frac{\chi^{\varepsilon}}{\Psi_{\bar{z}}} > 0. \tag{A.4}$$

Applying the chain rule, we derive the responses for the retail price, consumption, and product market tightness:

$$p_{\mu} = P_{\bar{z}}\bar{z}_{\mu} > 0, \quad c_{\mu} = lS_{\bar{z}}\bar{z}_{\mu} > 0, \quad \theta_{\mu} = \Theta_{\bar{z}}\bar{z}_{\mu} > 0.$$

Recall that spare capacity is defined as $\kappa \equiv l - c$, implying $\kappa_{\mu} = -c_{\mu} < 0$. Finally, the wholesale price is given by $r(z) = \eta p + \eta\rho\theta + (1-\eta)z$. Holding the realization of transportation cost z fixed, we obtain:

$$r_{\mu} = \eta p_{\mu} + \eta\rho\theta_{\mu} > 0.$$

[1] Note that the steady state exists only for $\bar{z} \geq \bar{z}_{\min}$.

A.3. Cross Derivatives

We first derive a general expression for the cross derivative applicable to any endogenous variable. Let ω denote a generic variable (e.g., $p, c,$ or θ) determined by the steady-state function $\Omega(\bar{z}, \gamma)$. We evaluate the cross derivative defined as $\omega_{\mu\gamma} \equiv \partial\omega_\mu/\partial\gamma$.

Recall that the baseline sensitivity to monetary policy is given by $\omega_\mu = \Omega_{\bar{z}}\bar{z}_\mu = \chi^\varepsilon\Omega_{\bar{z}}/\Psi_{\bar{z}}$. Taking natural logarithms yields:

$$\ln\omega_\mu = \varepsilon\ln\chi + \ln\Omega_{\bar{z}}(\bar{z},\gamma) - \ln\Psi_{\bar{z}}(\bar{z},\gamma).$$

Differentiating with respect to γ and invoking the assumption of short-run rigidity in the reservation threshold (i.e., $d\bar{z}^*/d\gamma = 0$) yields the general condition:

$$\frac{1}{\omega_\mu}\omega_{\mu\gamma} = \underbrace{\left(\frac{\partial\ln\Omega_{\bar{z}}}{\partial\bar{z}} - \frac{\partial\ln\Psi_{\bar{z}}}{\partial\bar{z}}\right)\frac{d\bar{z}^*}{d\gamma}}_{=0} + \frac{\partial\ln\Omega_{\bar{z}}}{\partial\gamma} - \frac{\partial\ln\Psi_{\bar{z}}}{\partial\gamma} = \frac{\partial\ln\Omega_{\bar{z}}}{\partial\gamma} - \frac{\partial\ln\Psi_{\bar{z}}}{\partial\gamma}.$$

Retail price. Applying the general condition to the retail price (where $\omega = p$ and $\Omega = P$), and given Condition (23) alongside the baseline result $p_\mu > 0$, it follows that:

$$p_{\mu\gamma} = p_\mu\left[\frac{\partial\ln P_{\bar{z}}}{\partial\gamma} - \frac{\partial\ln\Psi_{\bar{z}}}{\partial\gamma}\right] > 0.$$

Consumption. Similarly, applying the condition to consumption (where $\Omega = S$) and utilizing Condition (23) alongside $c_\mu > 0$, we derive:

$$c_{\mu\gamma} = c_\mu\left[\frac{\partial\ln S_{\bar{z}}}{\partial\gamma} - \frac{\partial\ln\Psi_{\bar{z}}}{\partial\gamma}\right] < 0.$$

Spare capacity. Since $\kappa_\mu = -c_\mu$, the cross derivative is given by:

$$\kappa_{\mu\gamma} = \frac{\partial}{\partial\gamma}(-c_\mu) = -c_{\mu\gamma} > 0.$$

Tightness. Applying the general condition to tightness (where $\Omega = \Theta$), the sign depends on the term $(\partial\ln\Theta_{\bar{z}}/\partial\gamma - \partial\ln\Psi_{\bar{z}}/\partial\gamma)$. Since Condition (23) does not impose restrictions on the sensitivity of $\Theta_{\bar{z}}$, the sign of $\theta_{\mu\gamma}$ is ambiguous.

Reservation transportation cost. From $\bar{z}_\mu = \chi^\varepsilon/\Psi_{\bar{z}}$, we obtain $\bar{z}_{\mu\gamma} = -\bar{z}_\mu\,(\partial\ln\Psi_{\bar{z}}/\partial\gamma)$. Since $\Psi_{\bar{z}}$ aggregates opposing effects ($P_{\bar{z}}$ rises while $S_{\bar{z}}$ falls), the sign is ambiguous.

Wholesale price. The response is given by $r_{\mu\gamma} = \eta p_{\mu\gamma} + \eta\rho\theta_{\mu\gamma}$. Although $p_{\mu\gamma} > 0$, the ambiguity of $\theta_{\mu\gamma}$ implies that the net effect on the wholesale price is ambiguous. ■

B. Monetary Policy Efficacy Under Capacity Constraints

In this appendix, we derive theoretical predictions regarding the efficacy of monetary policy in stabilizing prices and output, conditional on the extent of productive capacity constraints. Stated briefly, compared to the findings for supply chain disruptions (Proposition 3), we find that contractionary monetary policy is still more effective at curbing pressures on retail prices —while exerting a smaller impact on output and spare capacity— when productive capacity is constrained, despite differences in the predictions on other endogenous variables including product market tightness.

Consistent with the theoretical framework in Section 3, we characterize the stance of monetary policy through the parameter of nominal money supply μ. The availability of productive resources is governed by the fixed-factor endowment of producers, l, where a lower l corresponds to a tighter capacity constraint.

Proposition 3′. *Define nominal aggregate supply as $\Psi(\bar{z}, l) \equiv P(\bar{z})S(\bar{z})l$, where $P(\bar{z})$ and $S(\bar{z})$ are implicit functions of the reservation transportation cost $\bar{z}$ corresponding to the retail price p and matching share $S \equiv f(\theta)G(\bar{z})/\left(1 - G(\bar{z}) + f(\theta)G(\bar{z})\right)$, respectively. Assume that (i) the nominal aggregate supply function is log-concave with respect to the cutoff (i.e., $\partial^2 \ln \Psi / \partial \bar{z}^2 < 0$), (ii) the retail price function is strictly convex (i.e., $P_{\bar{z}\bar{z}} > 0$), and (iii) the matching share function is strictly concave (i.e., $S_{\bar{z}\bar{z}} < 0$).*

Accordingly, the cross derivatives describing the state-dependent interaction between monetary policy and capacity constraints are:

$$c_{\mu l} > 0, \quad p_{\mu l} < 0, \quad \kappa_{\mu l} < 0, \quad \theta_{\mu l} < 0, \quad r_{\mu l} < 0, \quad \bar{z}_{\mu l} < 0,$$

where $c, p, \kappa, \theta, r,$ and $\bar{z}$ denote consumption (equivalently, output), retail price, spare capacity, product market tightness, wholesale price, and reservation transportation cost, respectively.

Proof. The proof proceeds by first deriving the comparative statics of the reservation transportation cost $\bar{z}$ with respect to the productive capacity l, followed by the derivation of the cross derivative of each endogenous variable with respect to monetary policy μ and capacity l.

Recall from the proof of Proposition 3 that the system can be reduced to a single-equation steady-state condition:

$$\Psi(\bar{z}, l) \equiv \psi(\bar{z})l = \chi^{\varepsilon}\mu,$$

where $\psi(\bar{z}) \equiv P(\bar{z})S(\bar{z})$. To find the response of the cutoff to a change in productive capacity, we implicitly differentiate the steady-state condition with respect to l:

$$\frac{d}{dl}(\psi(\bar{z})l) = \psi'(\bar{z})\frac{d\bar{z}}{dl}l + \psi(\bar{z}) = 0.$$

Rearranging for $\bar{z}_l$ yields:

$$\bar{z}_l = -\frac{\psi(\bar{z})}{l\psi'(\bar{z})}.$$

Since $P(\bar{z})$ and $S(\bar{z})$ are strictly positive (see Equations (A.2) and (A.3)), the numerator satisfies $\psi(\bar{z}) > 0$. Regarding the denominator, the derivative is given by $\psi'(\bar{z}) = P_{\bar{z}}S + PS_{\bar{z}}$. Given that $P_{\bar{z}} > 0$ and $S_{\bar{z}} > 0$ (as established in the previous proof), it follows that $\psi'(\bar{z}) > 0$. Consequently, we obtain $\bar{z}_l < 0$.

Reservation transportation cost. Recall from Equation (A.4) that the sensitivity of the cutoff to the nominal money supply is $\bar{z}_\mu = \chi^{\varepsilon}/(l\psi'(\bar{z}))$. Differentiating with respect to l using the quotient rule yields:

$$\bar{z}_{\mu l} \equiv \frac{\partial \bar{z}_\mu}{\partial l} = -\frac{\chi^{\varepsilon}}{(l\psi')^2}\left(\psi' + l\psi''\bar{z}_l\right).$$

Substituting the capacity response $\bar{z}_l = -\psi/(l\psi')$ gives:

$$\bar{z}_{\mu l} = -\frac{\chi^{\varepsilon}}{(l\psi')^2}\left[\psi' + l\psi''\left(-\frac{\psi}{l\psi'}\right)\right] = -\frac{\chi^{\varepsilon}}{l\psi'}\frac{1}{l}\left[1 - \frac{\psi\psi''}{(\psi')^2}\right].$$

Substituting back the expression for $\bar{z}_\mu$, we obtain:

$$\bar{z}_{\mu l} = -\frac{\bar{z}_\mu}{l}\left[1 - \frac{\psi\psi''}{(\psi')^2}\right].$$

Condition (i) states that $\Psi(\bar{z})$ is log-concave with respect to $\bar{z}$. Since $\ln\Psi(\bar{z}) = \ln\psi(\bar{z}) + \ln l$, this implies that $\ln\psi(\bar{z})$ is strictly concave. Calculating the second derivative:

$$\frac{d^2}{d\bar{z}^2}\ln\psi(\bar{z}) = \frac{d}{d\bar{z}}\left(\frac{\psi'}{\psi}\right) = \frac{\psi''\psi - (\psi')^2}{\psi^2} < 0.$$

Since $\psi^2 > 0$, the numerator must be negative, implying $\psi''\psi < (\psi')^2$. Dividing by $(\psi')^2 > 0$ yields $\psi\psi''/(\psi')^2 < 1$. Consequently, the bracketed term $[1 - \psi\psi''/(\psi')^2]$ is strictly positive. Given

that $\bar{z}_\mu > 0$ and $l > 0$, we conclude that $\bar{z}_{\mu l} < 0$.

Retail price. Using the chain rule, the price sensitivity is given by $p_\mu = P_{\bar{z}}(\bar{z})\bar{z}_\mu$. Differentiating with respect to l yields:

$$p_{\mu l} \equiv \frac{\partial p_\mu}{\partial l} = P_{\bar{z}\bar{z}}\bar{z}_l\bar{z}_\mu + P_{\bar{z}}\bar{z}_{\mu l}.$$

The first term is negative because $P_{\bar{z}\bar{z}} > 0$ by Condition (ii), $\bar{z}_l < 0$ as derived above, and $\bar{z}_\mu > 0$. The second term is negative because $P_{\bar{z}} > 0$ and $\bar{z}_{\mu l} < 0$. Consequently, the total cross derivative is strictly negative, $p_{\mu l} < 0$.

Consumption. Recall that $c_\mu = lS_{\bar{z}}\bar{z}_\mu$. Substituting $\bar{z}_\mu = \chi^\varepsilon / [l\,(PS_{\bar{z}} + P_{\bar{z}}S)]$, we obtain the consumption sensitivity $c_\mu = \chi^\varepsilon / D(\bar{z})$, where the denominator is defined as:

$$D(\bar{z}) = P(\bar{z}) + S(\bar{z})\frac{P_{\bar{z}}(\bar{z})}{S_{\bar{z}}(\bar{z})}.$$

Differentiating $D(\bar{z})$ with respect to $\bar{z}$:

$$D'(\bar{z}) = P_{\bar{z}} + \left[S_{\bar{z}}\left(\frac{P_{\bar{z}}}{S_{\bar{z}}}\right) + S\frac{d}{d\bar{z}}\left(\frac{P_{\bar{z}}}{S_{\bar{z}}}\right)\right].$$

Applying the quotient rule to the last term yields:

$$D'(\bar{z}) = 2P_{\bar{z}} + S\left[\frac{P_{\bar{z}\bar{z}}S_{\bar{z}} - P_{\bar{z}}S_{\bar{z}\bar{z}}}{(S_{\bar{z}})^2}\right].$$

Rearranging the terms inside the bracket:

$$D'(\bar{z}) = 2P_{\bar{z}} + \frac{S}{S_{\bar{z}}}\left(P_{\bar{z}\bar{z}} - P_{\bar{z}}\frac{S_{\bar{z}\bar{z}}}{S_{\bar{z}}}\right).$$

Since $P_{\bar{z}}, S_{\bar{z}} > 0$, and by Conditions (ii) and (iii) where $P_{\bar{z}\bar{z}} > 0$ and $S_{\bar{z}\bar{z}} < 0$, the term in the parentheses is positive. Furthermore, as $S > 0$, the entire expression $D'(\bar{z})$ is strictly positive. Now, differentiating c_μ with respect to l yields:

$$c_{\mu l} \equiv \frac{\partial c_\mu}{\partial l} = -\frac{\chi^\varepsilon}{(D(\bar{z}))^2}D'(\bar{z})\bar{z}_l.$$

Given that $D'(\bar{z}) > 0$ and $\bar{z}_l < 0$, the total cross derivative is strictly positive, $c_{\mu l} > 0$.

Spare capacity. Since spare capacity is defined as $\kappa = l - c$, it follows that $\kappa_\mu = -c_\mu$. Therefore, the cross derivative is $\kappa_{\mu l} = -c_{\mu l} < 0$.

Tightness. Before delving into the cross derivative of θ, it is useful to derive the link between p and θ. Equation (A.1) implies the relationship:

$$\beta I(\bar{z}) = \frac{\rho}{(1-\eta)q(\theta)},$$

where $I(\bar{z}) \equiv \int_0^{\bar{z}} G(z')dz'$. Substituting this into Equation (A.2) and utilizing the identity $f(\theta)/q(\theta) = \theta$, we obtain:

$$P(\bar{z}) = \bar{z} - \beta I(\bar{z}) + \frac{\eta\rho}{1-\eta}\Theta(\bar{z}).$$

Differentiating twice with respect to $\bar{z}$ yields:

$$P_{\bar{z}\bar{z}} = -\beta G'(\bar{z}) + \frac{\eta\rho}{1-\eta}\Theta_{\bar{z}\bar{z}}.$$

Since the density function satisfies $G'(\bar{z}) > 0$, the term $-\beta G'(\bar{z})$ is negative. Hence, for $P_{\bar{z}\bar{z}} > 0$ to hold (per Condition (ii)), it must be that $[\eta\rho/(1-\eta)]\Theta_{\bar{z}\bar{z}} > \beta G' > 0$, which implies $\Theta_{\bar{z}\bar{z}} > 0$. Subsequently, differentiating the tightness sensitivity $\theta_\mu = \Theta_{\bar{z}}\bar{z}_\mu$ with respect to l yields:

$$\theta_{\mu l} \equiv \frac{\partial \theta_\mu}{\partial l} = \Theta_{\bar{z}\bar{z}}\bar{z}_l\bar{z}_\mu + \Theta_{\bar{z}}\bar{z}_{\mu l}.$$

Both terms on the right-hand side are negative, as $\Theta_{\bar{z}\bar{z}} > 0$, $\bar{z}_l < 0$, $\bar{z}_\mu > 0$, $\Theta_{\bar{z}} > 0$, and $\bar{z}_{\mu l} < 0$. Thus, we conclude that $\theta_{\mu l} < 0$.

Wholesale price. Recall from the comparative statics that the wholesale price sensitivity is $r_\mu = \eta p_\mu + \eta\rho\theta_\mu$. Differentiating with respect to l yields:

$$r_{\mu l} \equiv \frac{\partial r_\mu}{\partial l} = \eta p_{\mu l} + \eta\rho\theta_{\mu l}.$$

As derived earlier, $p_{\mu l} < 0$ and $\theta_{\mu l} < 0$. Since the parameters satisfy $\eta, \rho > 0$, the sum is strictly negative, implying $r_{\mu l} < 0$.

■

C. Data Sources

Table C.1 provides details on the data used in Sections 2 and 4, including sources and any construction or adjustment processes. Below, we provide further details on the construction of the spare capacity rate and the dollar-valued spare capacity used for product market tightness. The data used for robustness checks are described in subsequent appendices.

Spare capacity rate. In the main text, we define the spare capacity rate as an import-weighted average of capacity utilization shortfalls across the top five U.S. trading partners, i.e., Mexico, Canada, China, Germany, and Japan. To implement such a measure, we first construct monthly industrial production (IP) indices from official month-over-month growth rates, chaining forward from January 2017 and normalizing the starting value to 100. For Mexico and Japan, monthly capacity utilization rates are available and used as reported. For Canada, China, and Germany, where capacity utilization is reported only quarterly, we interpolate to a monthly frequency using the Chow–Lin method (Chow and Lin, 1971) with the chained monthly IP series as indicators. We then compute the spare capacity rate for each country as $100 - \text{CapacityUtilization}_t$ and aggregate these rates using weights proportional to each country's share of U.S. imports. We seasonally adjust the resulting series using the X-13ARIMA-SEATS algorithm provided by the U.S. Census Bureau.

Product market tightness. Tightness is defined as the ratio of U.S. manufacturers' new orders to the import-weighted value of spare capacity of major U.S. trading partners. The numerator, U.S. manufacturers' new orders, is readily available from FRED.

The denominator (spare capacity in U.S. dollar terms) requires a distinct construction to ensure unit consistency with new orders. Because the IP indices are unit-less, we first convert them into levels of production in U.S. dollars. We do this by anchoring the indices to annual data from the World Bank: we scale each country's monthly index series so that its aggregated annual value matches the country's reported industrial value added in constant U.S. dollars.

Once we have the monthly production levels in dollars, we estimate the dollar value of spare capacity, calculated as the constant dollar level of production multiplied by the ratio of unused capacity to utilized capacity. Conceptually, this measure represents the additional dollar value of goods that could be produced if capacity utilization increased to 100%. Finally, we aggregate these values using U.S. import shares as weights and seasonally adjust the final series.

Table C.1: Data Description and Sources

Variable	Mnemonic	Source	Notes on Construction/Adjustment
U.S. Variables			
Real GDP	GDPC1	U.S. Bureau of Economic Analysis	Quarterly series interpolated to monthly frequency using IP.
IP	INDPRO	Board of Governors of the Federal Reserve System	Raw series obtained directly from FRED.
PCE goods price index	DGDSRG3M086SBEA	U.S. Bureau of Economic Analysis	Raw series obtained directly from FRED.
Total manufacturers' new orders	AMTMNO	U.S. Census Bureau	Raw series obtained directly from FRED.
Imports of goods: Mexico	IMPMX	U.S. Census Bureau	Raw series obtained directly from FRED.
Imports of goods: Canada	IMPCA	U.S. Census Bureau	Raw series obtained directly from FRED.
Imports of goods: China	IMPCH	U.S. Census Bureau	Raw series obtained directly from FRED.
Imports of goods: Germany	IMPGE	U.S. Census Bureau	Raw series obtained directly from FRED.
Imports of goods: Japan	IMPJP	U.S. Census Bureau	Raw series obtained directly from FRED.
Import price index: all commodities	IR	U.S. Bureau of Labor Statistics	Seasonally adjusted by authors (X-13ARIMA-SEATS).
Federal funds effective rate	FEDFUNDS	Board of Governors of the Federal Reserve System	Raw series obtained directly from FRED.
ACR	N/A	Bai et al. (2023, 2024)	Seasonally adjusted by authors (X-13ARIMA-SEATS).
Variables for Top U.S. Trading Partners			
Capacity utilization rate: Mexico	N/A	National Institute of Statistics and Geography	Official monthly series..
Capacity utilization rate: Canada	N/A	Statistics Canada	Quarterly series interpolated to monthly frequency using IP.
Capacity utilization rate: China	N/A	National Bureau of Statistics of China	Quarterly series interpolated to monthly frequency using IP.
Capacity utilization rate: Germany	N/A	European Commission	Quarterly series interpolated to monthly frequency using IP.
Capacity utilization rate: Japan	N/A	Ministry of Economy, Trade and Industry	Official monthly series.
IP MoM growth: Mexico	N/A	National Institute of Statistics and Geography	Monthly series from official source.
IP MoM growth: Canada	N/A	Statistics Canada	Monthly series from official source.
IP MoM growth: China	N/A	National Bureau of Statistics of China	Monthly series from official source.
IP MoM growth: Germany	N/A	Federal Statistical Office	Monthly series from official source.
IP MoM growth: Japan	N/A	Ministry of Economy, Trade and Industry	Monthly series from official source.
IP: Mexico	N/A	World Bank	Annual series from World Development Indicators.
IP: Canada	N/A	World Bank	Annual series from World Development Indicators.
IP: China	N/A	World Bank	Annual series from World Development Indicators.
IP: Germany	N/A	World Bank	Annual series from World Development Indicators.
IP: Japan	N/A	World Bank	Annual series from World Development Indicators.

D. Robustness of Motivating Facts

To assess the robustness of Facts II and III in Section 2, we employ U.S. retailers' new orders as an alternative proxy for goods demand. We calculate the implied dollar value of these orders using the identity that orders equal the change in inventory plus sales:

$$\begin{aligned} \text{RetailNewOrder}_t &= \left(\text{Inventory}_t - \text{Inventory}_{t-1}\right) + \text{Sales}_t \\ &= \left(\text{Inventory}_t - \text{Inventory}_{t-1}\right) + \left(\frac{\text{Inventory}_t}{\text{Sales}_t}\right)^{-1} \cdot \text{Inventory}_t, \end{aligned} \tag{D.1}$$

where Inventory_t denotes the inventories held by U.S. retailers and $\text{Inventory}_t/\text{Sales}_t$ represents the inventory-to-sales ratio. Their monthly time series are obtained from FRED using the mnemonics `RETAILIMSA` and `RETAILIRSA`, respectively.

Figure D.1 compares this derived measure of U.S. retailers' new orders with the import-weighted average spare capacity of the top five U.S. trading partners (Mexico, Canada, China, Germany, and Japan). The figure confirms that Fact II remains robust: a significant and persistent wedge between domestic demand and global spare capacity emerges following the onset of the COVID-19 pandemic.

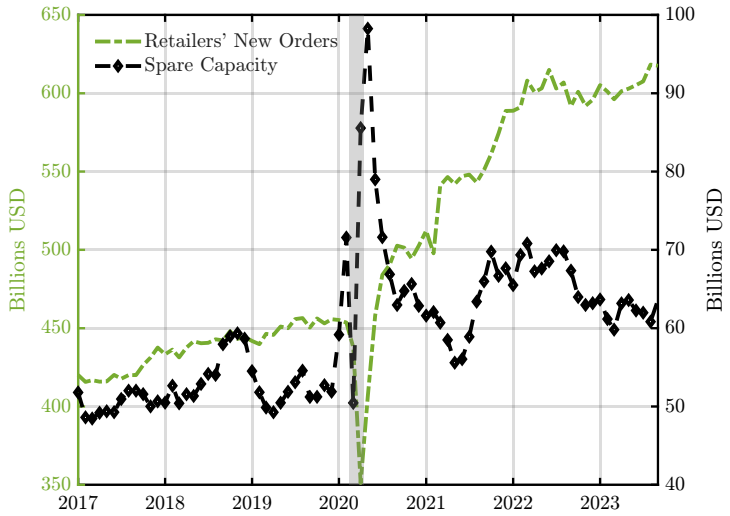

Figure D.1: Imbalances in the Supply and Demand for Goods: U.S. Retailers' New Orders

Notes. The figure compares U.S. retailers' new orders, constructed using Equation (D.1), with the import-weighted average spare capacity of the specified U.S. trading partners, calculated using Equation (1). Both series are measured in billions of U.S. dollars and seasonally adjusted.

Next, we substitute total U.S. manufacturers' new orders with this retailer-based measure to

construct an alternative index of product market tightness:

$$\text{AlternativeTightness}_t = \frac{\text{RetailNewOrder}_t}{\text{SpareCapacityDollar}_t}, \tag{D.2}$$

where $\text{SpareCapacityDollar}_t$ is the import-weighted average spare capacity (Equation (1)).

Figure D.2 plots this alternative tightness measure against the U.S. PCE goods price index. The two series exhibit strong co-movement following the onset of the pandemic, confirming the robustness of Fact III: goods prices surged alongside the tightening of the product market.

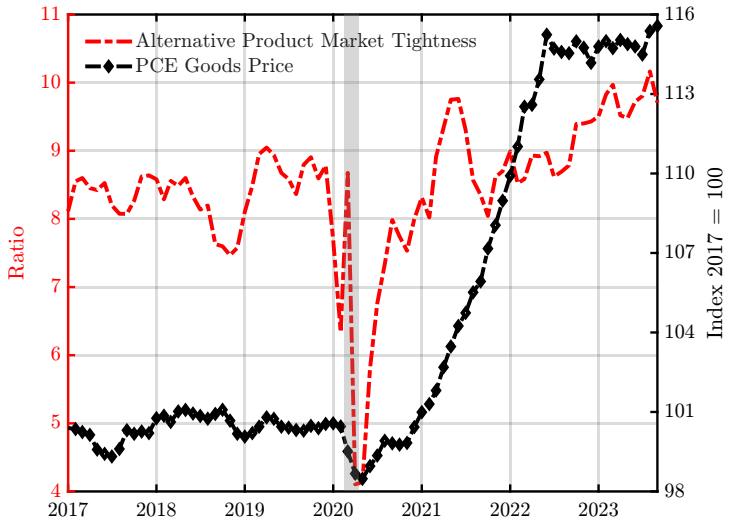

Figure D.2: Co-Movements Between Goods Prices and Alternative Measure of Tightness

Notes. The figure compares the U.S. PCE goods price with an alternative measure of product market tightness, calculated using Equation (D.2). The PCE goods price is presented in its original units, and the alternative measure of product market tightness is expressed as a ratio. Both series are seasonally adjusted.

E. Priors and Identification in the TVAR

E.1. Priors

Our formulation of the prior in the TVAR model follows Bańbura et al. (2010), Mumtaz and Zanetti (2012), and Pizzinelli et al. (2020). We apply the same prior to the parameters in both the supply chain disrupted ($\mathbb{D}$) and undisrupted ($\mathbb{U}$) regimes. Specifically, we write the TVAR model in Equation (24) compactly as a system of multivariate regressions:

$$\boldsymbol{y} = (\boldsymbol{M}_{\mathbb{D}}\boldsymbol{x}_{\mathbb{D}} + \boldsymbol{u}_{\mathbb{D}})\boldsymbol{I} + (\boldsymbol{M}_{\mathbb{U}}\boldsymbol{x}_{\mathbb{U}} + \boldsymbol{u}_{\mathbb{U}})(\boldsymbol{1}_{T\times T} - \boldsymbol{I}), \tag{E.1}$$

where $\boldsymbol{y} = [\boldsymbol{y}_1 \ \dots \ \boldsymbol{y}_T]$ is an $n \times T$ matrix; $\boldsymbol{x}_{\mathbb{D}} = [\boldsymbol{x}_{\mathbb{D},1} \ \dots \ \boldsymbol{x}_{\mathbb{D},T}]$ is an $m \times T$ matrix with $\boldsymbol{x}_{\mathbb{D},t} = [\boldsymbol{y}'_{t-1} \ \dots \ \boldsymbol{y}'_{t-L} \ \boldsymbol{\omega}'_t]'$, $\boldsymbol{\omega}_t = [1, t]'$, and $m = nL+2$; $\boldsymbol{x}_{\mathbb{U}}$ is defined similarly; $\boldsymbol{u}_{\mathbb{D}} = [\boldsymbol{\Sigma}_{\mathbb{D}}^{1/2}\boldsymbol{\epsilon}_1 \ \dots \ \boldsymbol{\Sigma}_{\mathbb{D}}^{1/2}\boldsymbol{\epsilon}_T]$ and $\boldsymbol{u}_{\mathbb{U}} = [\boldsymbol{\Sigma}_{\mathbb{U}}^{1/2}\boldsymbol{\epsilon}_1 \ \dots \ \boldsymbol{\Sigma}_{\mathbb{U}}^{1/2}\boldsymbol{\epsilon}_T]$ are $n \times T$ error matrices; $\boldsymbol{\Sigma}_{\mathbb{D}}$ and $\boldsymbol{\Sigma}_{\mathbb{U}}$ are the variance-covariance matrices; $\boldsymbol{I} = \text{diag}[I_1 \ \dots \ I_T]$ is a $T \times T$ diagonal indicator matrix; and $\boldsymbol{M}_{\mathbb{D}} = [\boldsymbol{B}'_{\mathbb{D},1} \ \dots \ \boldsymbol{B}'_{\mathbb{D},L} \ \boldsymbol{C}'_{\mathbb{D}}]$ and $\boldsymbol{M}_{\mathbb{U}} = [\boldsymbol{B}'_{\mathbb{U},1} \ \dots \ \boldsymbol{B}'_{\mathbb{U},L} \ \boldsymbol{C}'_{\mathbb{U}}]$ are $n \times m$ matrices of coefficients.

Given Equation (E.1), for each regime $r \in \{\mathbb{D}, \mathbb{U}\}$, we assume the parameter vector, $\text{vec}(\boldsymbol{M}_r)$, follows a Normal-Inverse-Wishart conjugate prior. This form is given by:

$$\text{vec}(\boldsymbol{M}_r)|\boldsymbol{\Sigma}_r \sim \mathcal{N}\left(\text{vec}(\boldsymbol{M}_r^0), \boldsymbol{\Sigma}_r \otimes \boldsymbol{\Omega}_r^0\right), \quad \boldsymbol{\Sigma}_r \sim \mathcal{IW}\left(\boldsymbol{S}_r^0, \alpha_r^0\right), \tag{E.2}$$

where $\text{vec}(\boldsymbol{M}_r^0)$ is the prior mean, $\boldsymbol{\Omega}_r^0$ controls the tightness, $\boldsymbol{S}_r^0$ is the prior scale matrix of the Inverse-Wishart ($\mathcal{IW}$) distribution, and α_r^0 denotes the degrees of freedom. Essentially, the prior in Equation (E.2) generalizes the Minnesota prior (Litterman, 1986) by assuming endogenous variables follow a random walk or an AR(1) process. This approach assigns greater weight to recent lags, reflecting the notion that they contain more reliable information about system dynamics. Unlike the original formulation, however, Equation (E.2) does not assume a fixed, diagonal variance-covariance matrix, making it more suitable for structural analysis.

The Normal-Inverse-Wishart prior implies that while the prior expectations and variances for the constant and linear trend, $\boldsymbol{C}_r$, are diffuse, those for the autoregressive matrices, $\boldsymbol{B}_{r,l}$, are:

$$\mathbb{E}[(\boldsymbol{B}_{r,l})_{i,j}] = \begin{cases} \beta_{r,i}^0, & \text{if } i = j, \ l = 1; \\ 0, & \text{otherwise;} \end{cases} \qquad \mathbb{V}[(\boldsymbol{B}_{r,l})_{i,j}] = \frac{\lambda^2\sigma_i^2}{l^2\sigma_j^2}, \tag{E.3}$$

where $\beta^0_{r,1}, \ldots, \beta^0_{r,n}$ are the prior means of the autoregressive coefficients, $\sigma_1, \ldots, \sigma_n$ are the prior error standard deviations, and the hyper-parameter λ controls overall tightness such that a larger λ implies a looser prior. As described in Bańbura et al. (2010), we implement these moments by adding $T_{r,d}$ dummy observations, $\boldsymbol{y}_{r,d}$ and $\boldsymbol{x}_{r,d}$, to the system of regressions in Equation (E.1) corresponding to each regime, with $\boldsymbol{y}_{r,d}$ and $\boldsymbol{x}_{r,d}$ satisfying:

$$\boldsymbol{y}_{r,d} = \begin{bmatrix} \text{diag}[\beta^0_{r,1}\sigma_1 \ \ldots \ \beta^0_{r,n}\sigma_n]/\lambda \\ \mathbf{0}_{n(L-1)\times n} \\ \text{diag}[\sigma_1 \ \ldots \ \sigma_n] \\ \mathbf{0}_{2\times n} \end{bmatrix}, \quad \boldsymbol{x}_{r,d} = \begin{bmatrix} J_L \otimes \text{diag}[\sigma_1 \ \ldots \ \sigma_n]/\lambda & \mathbf{0}_{nL\times 1} & \mathbf{0}_{nL\times 1} \\ \mathbf{0}_{n\times nL} & \mathbf{0}_{n\times 1} & \mathbf{0}_{n\times 1} \\ \mathbf{0}_{1\times nL} & \xi & 0 \\ \mathbf{0}_{1\times nL} & 0 & \xi \end{bmatrix},$$

where $J_L = \text{diag}[1 \ \ldots \ L]$ and ξ controls the informativeness of the prior on the deterministic terms. The prior moments in Equation (E.2) are then defined as:

$$\boldsymbol{M}^0_r = \boldsymbol{y}_{r,d}\boldsymbol{x}'_{r,d}(\boldsymbol{x}_{r,d}\boldsymbol{x}'_{r,d})^{-1}, \quad \boldsymbol{\Omega}^0_r = (\boldsymbol{x}_{r,d}\boldsymbol{x}'_{r,d})^{-1},$$
$$\boldsymbol{S}^0_r = (\boldsymbol{y}_{r,d} - \boldsymbol{M}^0_r\boldsymbol{x}_{r,d})(\boldsymbol{y}_{r,d} - \boldsymbol{M}^0_r\boldsymbol{x}_{r,d})', \quad \alpha^0_r = T_{r,d} - m.$$

Since the Normal-Inverse-Wishart prior is conjugate, the conditional posterior distribution is also Normal-Inverse-Wishart (Kadiyala and Karlsson, 1997; Bańbura et al., 2010):

$$\text{vec}(\boldsymbol{M}_r)|\boldsymbol{\Sigma}_r, \boldsymbol{y} \sim \mathcal{N}\left(\text{vec}(\tilde{\boldsymbol{M}}_r), \boldsymbol{\Sigma}_r \otimes (\tilde{\boldsymbol{x}}_r\tilde{\boldsymbol{x}}'_r)^{-1}\right), \quad \boldsymbol{\Sigma}_r|\boldsymbol{y} \sim \mathcal{IW}\left(\tilde{\boldsymbol{S}}_r, T_{r,d} + 2 + T - m\right),$$

where the posterior parameters are:

$$\tilde{\boldsymbol{M}}_r = \tilde{\boldsymbol{y}}_r\tilde{\boldsymbol{x}}'_r(\tilde{\boldsymbol{x}}_r\tilde{\boldsymbol{x}}'_r)^{-1}, \quad \tilde{\boldsymbol{S}}_r = (\tilde{\boldsymbol{y}}_r - \tilde{\boldsymbol{M}}_r\tilde{\boldsymbol{x}}_r)(\tilde{\boldsymbol{y}}_r - \tilde{\boldsymbol{M}}_r\tilde{\boldsymbol{x}}_r)'.$$

Here, $\tilde{\boldsymbol{y}}_r$ and $\tilde{\boldsymbol{x}}_r$ represent the matrices $\boldsymbol{y}_r$ and $\boldsymbol{x}_r$ augmented with the dummy observations $\boldsymbol{y}_{r,d}$ and $\boldsymbol{x}_{r,d}$, respectively.[2]

Following Mumtaz and Zanetti (2012) and Pizzinelli et al. (2020), we obtain the prior means $\beta^0_{r,i}$ and error standard deviations σ_i via OLS estimation of a univariate AR(1) model for each endogenous variable. In the baseline estimation, we set $\lambda = 0.25$ to ensure fast lag decay.

Finally, we assume $\overline{\text{ACR}}$ is normally distributed, with its mean at the median of the ACR series and its standard deviation calibrated to achieve a Markov Chain Monte Carlo acceptance rate of approximately 70% to 75%.

[2] $\boldsymbol{y}_r$ denotes the subset of $\boldsymbol{y}$ associated with regime $r \in \{\mathbb{D}, \mathbb{U}\}$.

E.2. Identification Using the PFA

Following Uhlig (2005) and Mountford and Uhlig (2009), the identification scheme we employ to study the state-dependent effects of a contractionary monetary policy shock amounts to finding an impulse vector $\boldsymbol{a}$ that minimizes a criterion function over the space of all possible impulse vectors. This function penalizes sign violations for real GDP, PCE goods price, product market tightness, import price, the federal funds rate, and the spare capacity rate at horizons $k = 0, \ldots, K$, while strictly satisfying the zero restriction imposed on the impact response of the ACR index.[3] The scheme is applied separately for the observations in each regime. Hence, for simplicity, we drop the regime-specific notation $r \in \{\mathbb{D}, \mathbb{U}\}$ in the following description.

The PFA is implemented numerically as a constrained minimization problem. Let $r_{j,\boldsymbol{a}}(k)$ denote the impulse response of variable j at horizon k to the shock defined by vector $\boldsymbol{a}$, and let σ_j be the standard deviation of variable j. We define the standardized impulse response as $\tilde{r}_{j,\boldsymbol{a}}(k) = r_{j,\boldsymbol{a}}(k)/\sigma_j$. Furthermore, let $s_j \in \{+1, -1\}$ denote the expected sign of the response for variable j under a contractionary monetary policy shock. Specifically, we set $s_j = +1$ for the federal funds rate and the spare capacity rate, and $s_j = -1$ for real GDP, PCE goods price, product market tightness, and import price.

To evaluate the adherence of a candidate vector $\boldsymbol{a}$ to these priors, we compute the signed agreement metric $x_{j,k} = s_j \cdot \tilde{r}_{j,\boldsymbol{a}}(k)$. The objective is to minimize the total loss $\mathscr{L}(\boldsymbol{a})$, defined as:

$$\mathscr{L}(\boldsymbol{a}) = \sum_{j \in \mathscr{J}} \sum_{k=0}^{K} g(x_{j,k}), \tag{E.4}$$

where $\mathscr{J}$ represents the set of constrained variables. The component penalty function $g(x)$ is defined as:

$$g(x) = \begin{cases} -\lambda_{\text{sign}} \cdot x, & \text{if } x \leq 0; \\ \lambda_{\text{inv}}/(x + \epsilon), & \text{if } x > 0, \end{cases}$$

where $\lambda_{\text{sign}} = 100$, $\lambda_{\text{inv}} = 1$, and $\epsilon = 10^{-4}$. This formulation imposes a heavy linear penalty on sign violations ($x \leq 0$) and an inverse-magnitude penalty on correct signs ($x > 0$). The latter term distinguishes our approach from pure sign-restriction methods by favoring responses that are not only correctly signed but also possess a magnitude distinct from zero.

[3] As shown in Figure F.4, our identification results using the PFA are also robust to removing the zero restriction imposed on the impact response of the ACR index.

We find the contractionary monetary policy vector for each draw from the posterior by minimizing Equation (E.4) subject to the hard constraint on the ACR index:

$$r_{\text{ACR},\boldsymbol{a}}(0) = 0.$$

This optimization is performed numerically using a sequential quadratic programming method. We record the optimal impulse vector for each posterior draw and compute the corresponding IRFs reported in the main text.

E.3. Posterior and Identified Regimes

Figure E.1 presents the estimation results for the regime-switching threshold. The left panel plots the posterior distribution of the threshold parameter, $\overline{\text{ACR}}$. The right panel displays the time series of the identified regimes, constructed using the median of this posterior distribution.

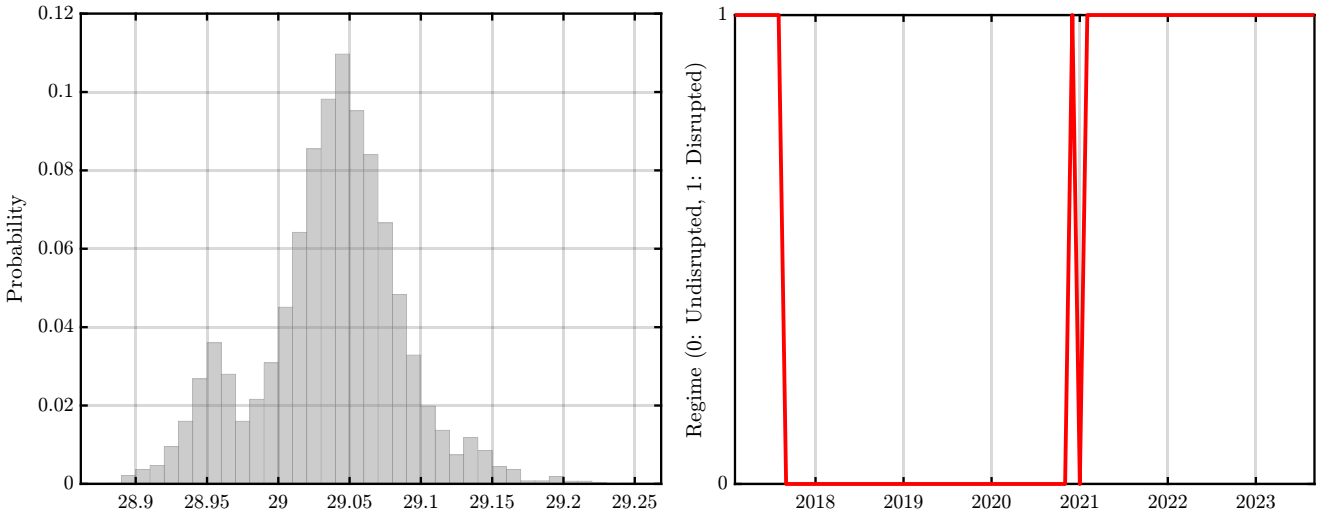

Figure E.1: Posterior Distribution of $\overline{\text{ACR}}$ and Identified Regimes

Notes. The left panel plots the posterior distribution of the regime-switching threshold, $\overline{\text{ACR}}$, based on 10,000 independent draws. In the right panel, the solid red line indicates the regime identified by the median of the posterior distribution of $\overline{\text{ACR}}$. A value of one corresponds to the supply chain disrupted ($\mathbb{D}$) regime, while a value of zero corresponds to the supply chain undisrupted ($\mathbb{U}$) regime.

F. Robustness of TVAR Results

This appendix presents robustness checks for the state-dependent effects of monetary contraction using several variations of the baseline TVAR specification. Figure F.1 confirms that our results persist when using the ACT index developed in our companion paper (Bai et al., 2024) to capture the state of the global supply chain. The ACT index measures the average number of hours a container ship waits in a port's anchorage before docking at a berth, weighted by the relative number of ship visits to each of the top 50 container ports worldwide.

Figure F.2 demonstrates robustness to using the Wu–Xia shadow federal funds rate (Wu and Xia, 2016), which estimates the effective rate during zero-lower-bound periods to capture the effects of unconventional monetary policy. Additionally, Figure F.3 shows that the results are invariant to an alternative measure of product market tightness defined in Equation (D.2), while Figure F.4 establishes robustness when relaxing the zero restriction on the impact response of the ACR index.

We also validate the model under alternative specifications. Figures F.5 and F.6 show that the results hold under different lag structures (two or three lags); models with four or more lags are excluded due to parameter uncertainty given the limited sample size. Figure F.7 confirms robustness to a looser estimation prior ($\lambda = 0.5$). Finally, Figure F.8 illustrates robustness to a parsimonious specification that includes only a constant.

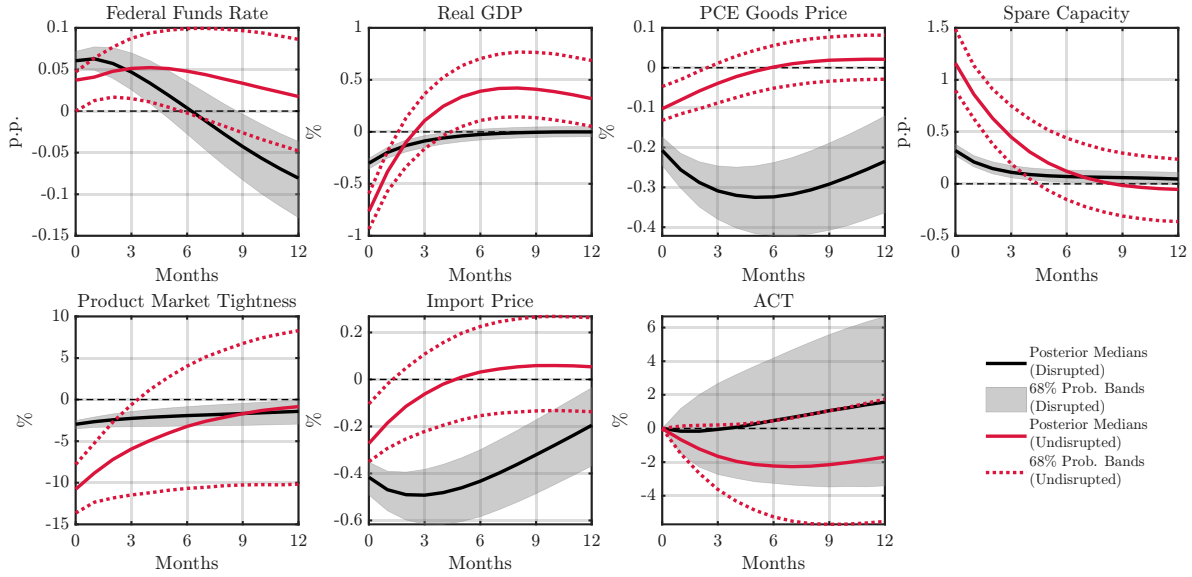

Figure F.1: State-Dependent Effects of Monetary Contraction (TVAR): ACT

Notes. The figure plots IRFs to a one-standard-deviation contractionary monetary policy shock identified using the Bayesian structural TVAR in Equation (24), with the ACT index (Bai et al., 2024) used to distinguish between supply chain disrupted and undisrupted states, and with Restriction 1 imposed on the impact responses of the endogenous variables. Solid black (red) lines denote pointwise posterior medians for the disrupted (undisrupted) regime, while shaded black areas (dotted red lines) depict the corresponding 68% equal-tailed posterior probability bands. Results are based on 10,000 independent posterior draws.

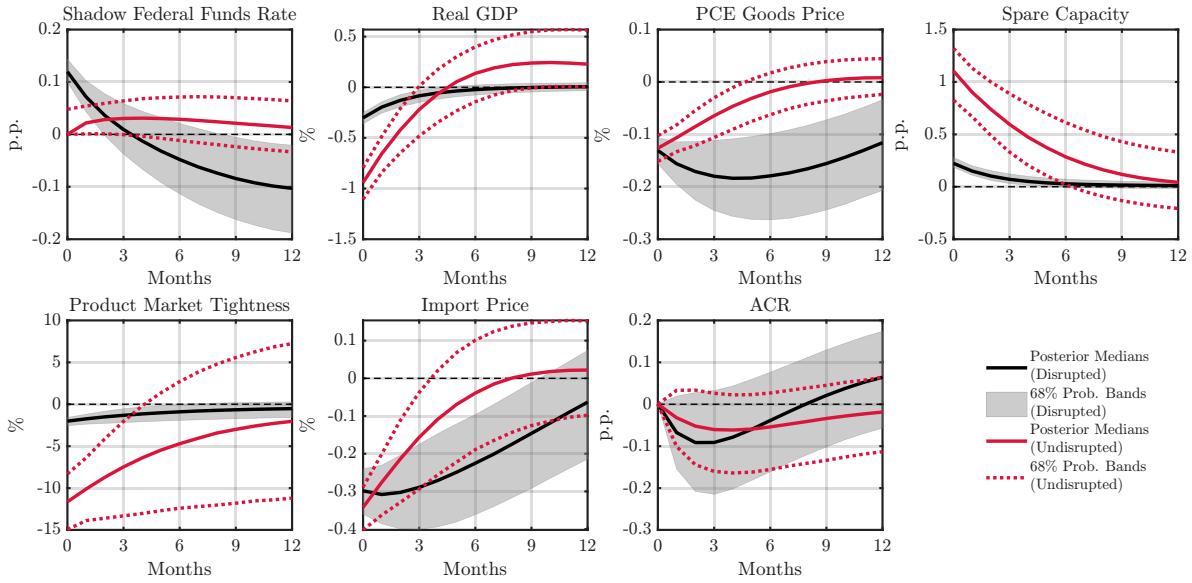

Figure F.2: State-Dependent Effects of Monetary Contraction (TVAR): Wu-Xia Shadow Federal Funds Rate

Notes. The figure plots IRFs using the Wu–Xia shadow federal funds rate (Wu and Xia, 2016) to reflect the stance of U.S. monetary policy. Notation follows Figure F.1: black (red) denotes the disrupted (undisrupted) regime, with solid lines representing posterior medians and shaded/dotted areas representing 68% posterior probability bands.

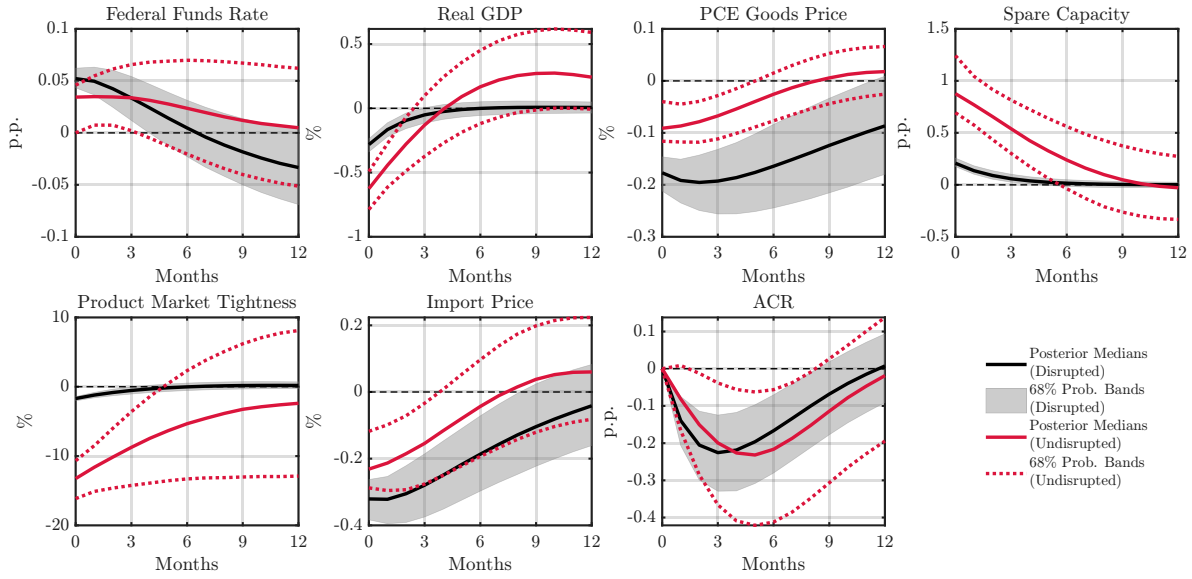

Figure F.3: State-Dependent Effects of Monetary Contraction (TVAR): Alternative Measure of Product Market Tightness

Notes. The figure plots IRFs with the alternative measure of product market tightness (D.2) included as an endogenous variable. Notation and probability bands follow Figure F.1.

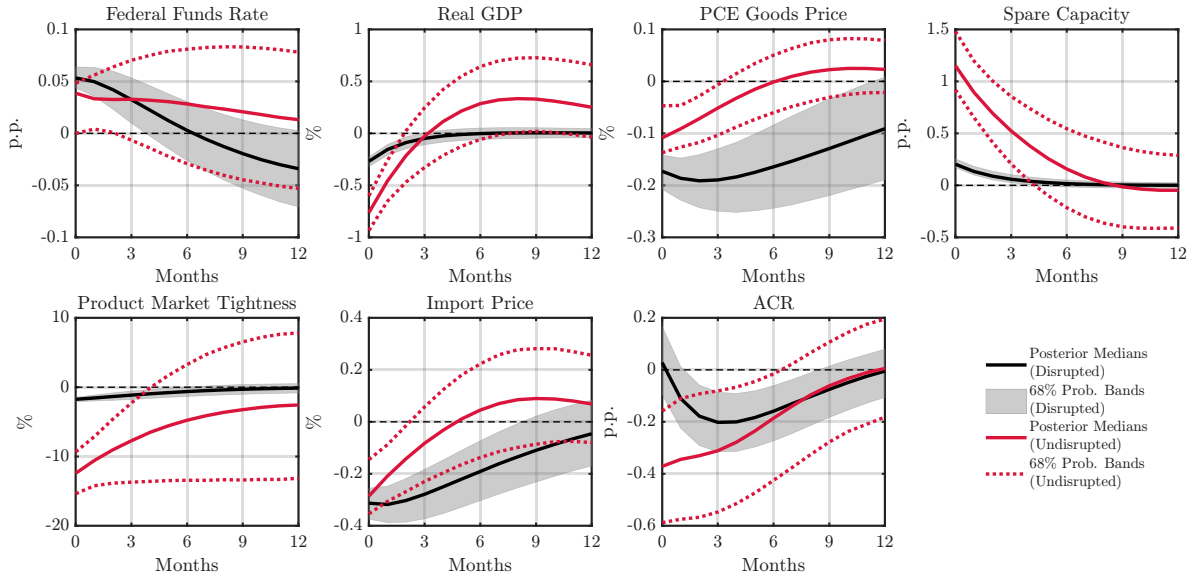

Figure F.4: State-Dependent Effects of Monetary Contraction (TVAR): No Zero Restriction

Notes. The figure plots IRFs to a contractionary monetary policy shock identified without imposing the zero restriction on the impact response of the ACR index. Notation and probability bands follow Figure F.1.

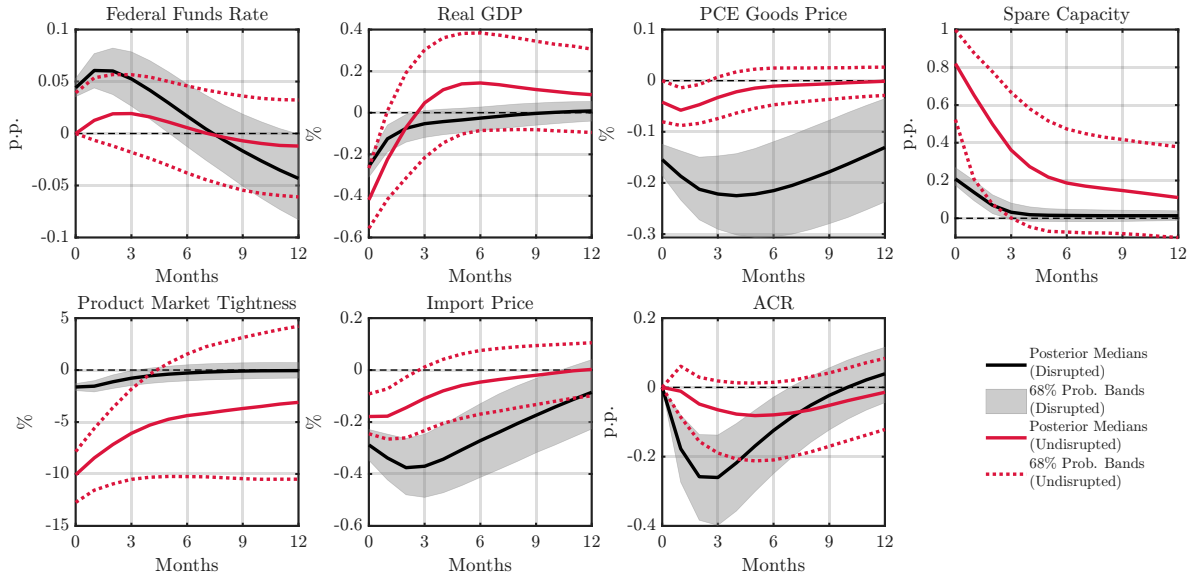

Figure F.5: State-Dependent Effects of Monetary Contraction (TVAR): Two Lags

Notes. The figure plots IRFs from the TVAR model estimated with two lags. Notation and probability bands follow Figure F.1.

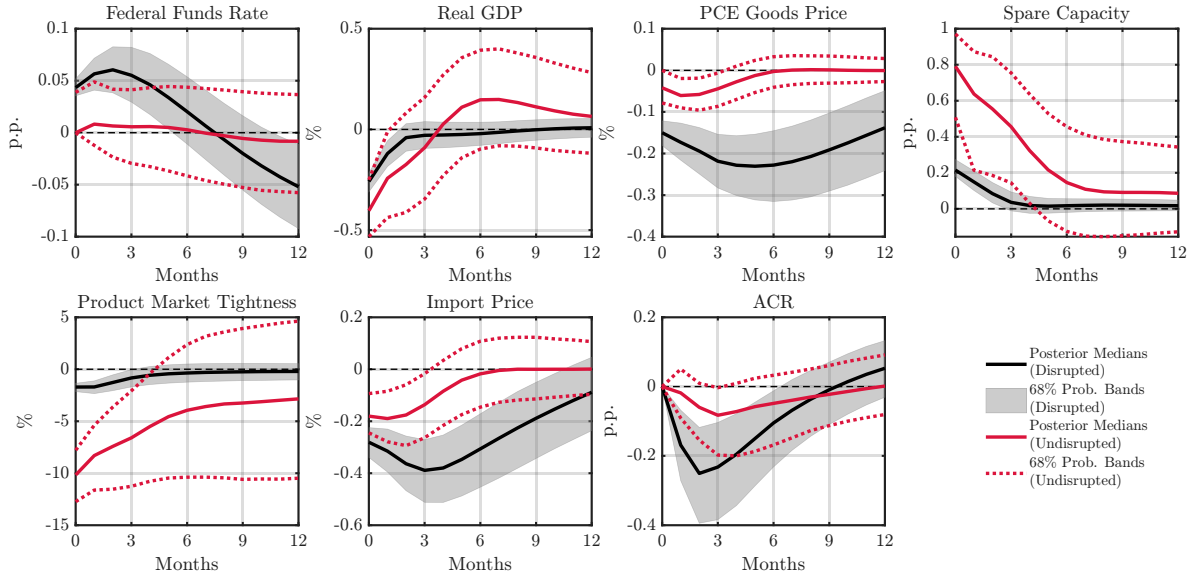

Figure F.6: State-Dependent Effects of Monetary Contraction (TVAR): Three Lags

Notes. The figure plots IRFs from the TVAR model estimated with three lags. Notation and probability bands follow Figure F.1.

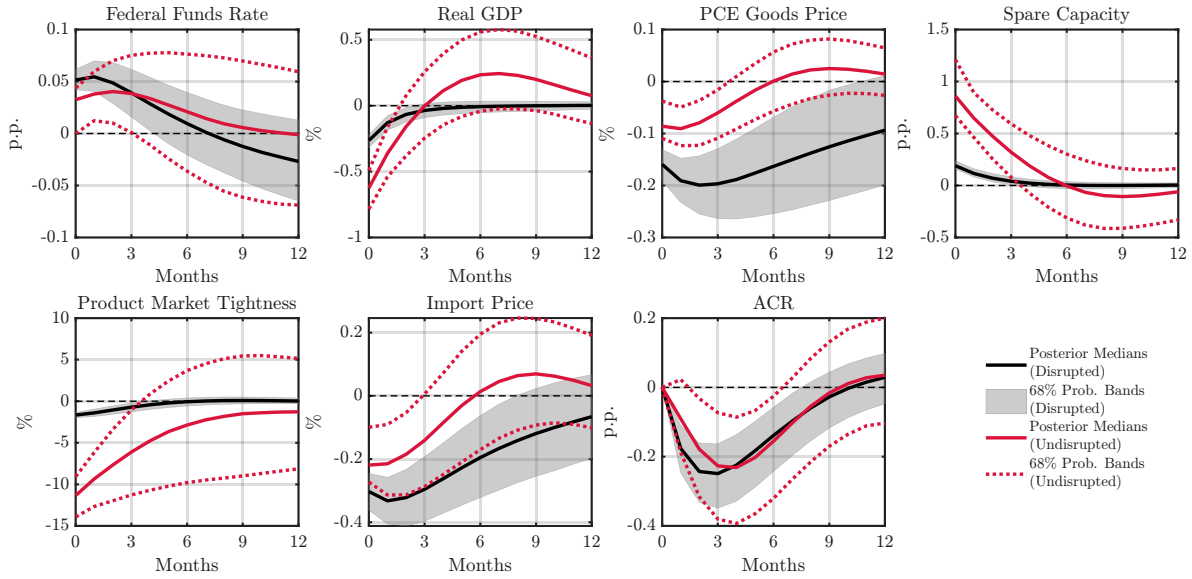

Figure F.7: State-Dependent Effects of Monetary Contraction (TVAR): Loose Prior

Notes. The figure plots IRFs from the TVAR model estimated with a looser prior ($\lambda = 0.5$). Notation and probability bands follow Figure F.1.

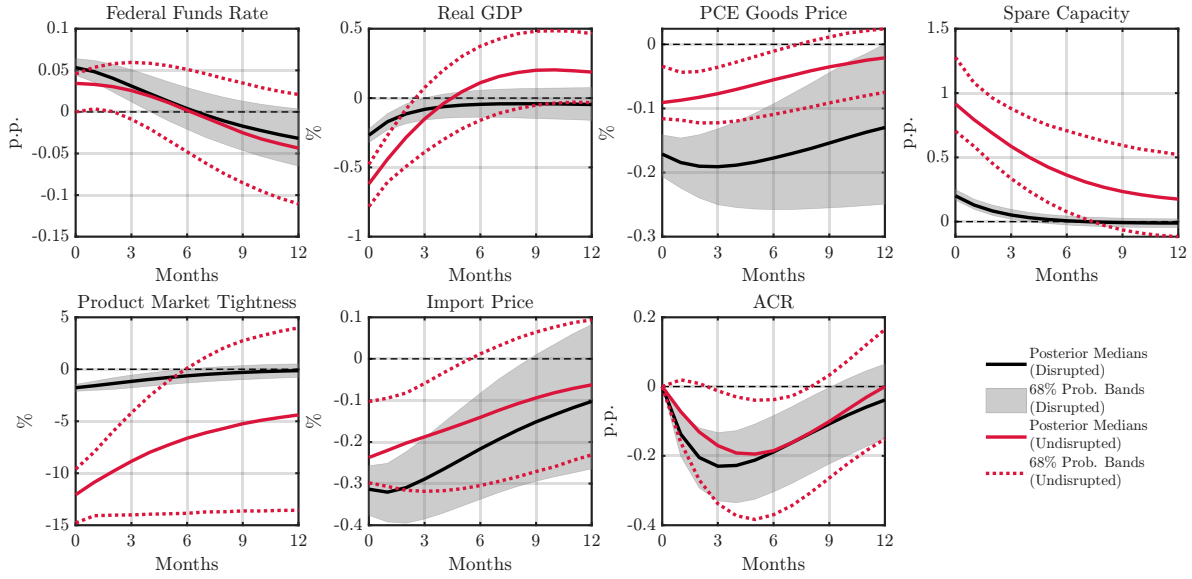

Figure F.8: State-Dependent Effects of Monetary Contraction (TVAR): Constant Only

Notes. The figure plots IRFs from a TVAR specification including only a constant (no trend). Notation and probability bands follow Figure F.1.

References for Appendices

Bai, X., Fernández-Villaverde, J., Li, Y., and Zanetti, F. (2024). The Causal Effects of Global Supply Chain Disruptions on Macroeconomic Outcomes: Evidence and Theory. Working Paper 32098, National Bureau of Economic Research.

Bai, X., Ma, Z., Hou, Y., Li, Y., and Yang, D. (2023). A Data-Driven Iterative Multi-Attribute Clustering Algorithm and Its Application in Port Congestion Estimation. *IEEE Transactions on Intelligent Transportation Systems*, 24:12026–12037.

Bańbura, M., Giannone, D., and Reichlin, L. (2010). Large Bayesian Vector Auto Regressions. *Journal of Applied Econometrics*, 25:71–92.

Chow, G. C. and Lin, A.-l. (1971). Best Linear Unbiased Interpolation, Distribution, and Extrapolation of Time Series by Related Series. *Review of Economics and Statistics*, 53:372–375.

Kadiyala, K. R. and Karlsson, S. (1997). Numerical Methods for Estimation and Inference in Bayesian VAR-Models. *Journal of Applied Econometrics*, 12(2):99–132.

Litterman, R. B. (1986). Forecasting With Bayesian Vector Autoregressions: Five Years of Experience. *Journal of Business & Economic Statistics*, 4:25–38.

Mountford, A. and Uhlig, H. (2009). What Are the Effects of Fiscal Policy Shocks? *Journal of Applied Econometrics*, 24:960–992.

Mumtaz, H. and Zanetti, F. (2012). Neutral Technology Shocks and the Dynamics of Labor Input: Results From an Agnostic Identification. *International Economic Review*, 53:235–254.

Pizzinelli, C., Theodoridis, K., and Zanetti, F. (2020). State Dependence in Labor Market Fluctuations. *International Economic Review*, 61:1027–1072.

Uhlig, H. (2005). What Are the Effects of Monetary Policy on Output? Results From an Agnostic Identification Procedure. *Journal of Monetary Economics*, 52:381–419.

Wu, J. C. and Xia, F. D. (2016). Measuring the Macroeconomic Impact of Monetary Policy at the Zero Lower Bound. *Journal of Money, Credit and Banking*, 48(2-3):253–291.